

BVRI Light Curves for 22 Type Ia Supernovae

Accepted to the Astronomical Journal

Adam G. Riess¹, Robert P. Kirshner², Brian P. Schmidt³, Saurabh Jha², Peter Challis², Peter M. Garnavich², Ann A. Esin², Chris Carpenter², Randy Grashius⁴, Rudolph E. Schild², Perry L. Berlind⁵, John P. Huchra², Charles F. Prosser⁶, Emilio E. Falco², Priscilla J. Benson⁷, Cesar Briceno², Warren R. Brown², Nelson Caldwell⁵, Ian P. Dell'Antonio⁸, Alexei V. Filippenko¹, Alyssa A. Goodman², Norman A. Grogan², Ted Groner⁵, John P. Hughes⁹, Paul J. Green², Rolf A. Jansen², Jan T. Kleyna², Jane X. Luu², Lucas M. Macri², Brian A. McLeod², Kim K. McLeod⁷, Brian R. McNamara², Brian McLean¹⁰, Alejandra A. E. Milone¹¹, Joseph J. Mohr¹², Dan Moraru², Chien Peng¹¹³, Jim Peters⁵, Andrea H. Prestwich², Krzysztof Z. Stanek², Ping Zhao²

ABSTRACT

We present 1210 Johnson/Cousins B,V,R, and I photometric observations of 22 recent type Ia supernovae (SNe Ia): SN 1993ac, SN 1993ae, SN 1994M, SN 1994S, SN 1994T, SN 1994Q, SN 1994ae, SN 1995D, SN 1995E, SN 1995al, SN 1995ac, SN 1995ak, SN 1995bd, SN 1996C, SN 1996X, SN 1996Z, SN 1996ab, SN 1996ai, SN 1996bk, SN 1996bl, SN 1996bo, and SN 1996bv.

¹Department of Astronomy, University of California, Berkeley, CA 94720-3411

²Harvard-Smithsonian Center for Astrophysics, 60 Garden St., Cambridge, MA 02138

³Mount Stromlo and Siding Spring Observatories, Private Bag, Weston Creek P.O. 2611, Australia

⁴University of New Mexico, Capilla Peak Observatory, Albuquerque, NM 87131

⁵Fred Lawrence Whipple Observatory, Amado, AZ 85645

⁶NOAO, Tucson, AZ 85726

⁷Whitin Observatory, Wellesley College, MA 02481-8203

⁸Bell Lab, Murray Hill, NJ 07974

⁹Rutgers University, Dept. of Physics & Astronomy, New Brunswick, NJ 08855

¹⁰Space Telescope Science Institute, Baltimore, MD 21218

¹¹Multiple Mirror Telescope Observatory, c/o Whipple Observatory, P.O. Box 97, Amado AZ 85645-0097

¹²Department of Astronomy and Astrophysics, University of Chicago, Chicago, IL 60637

¹³Steward Observatory, University of Arizona, Tucson, AZ 85721

Most of the photometry was obtained at the Fred Lawrence Whipple Observatory (FLWO) of the Harvard-Smithsonian Center for Astrophysics in a cooperative observing plan aimed at improving the data base for SN Ia. The redshifts of the sample range from $cz=1200$ to 37000 km s^{-1} with a mean of $cz=7000 \text{ km s}^{-1}$.

1. Introduction

Recent evidence suggests that type Ia supernovae (SNe Ia) can be used as exceedingly precise long-range distance indicators (Riess, Press, & Kirshner 1995a,b, 1996a,b; Hamuy et al. 1995, 1996a,b; Maza et al. 1994; Phillips 1993; Tammann & Sandage 1995). With peak luminosities a million times greater than Cepheid variables and individual distance accuracy approaching 5%, they provide cosmology with a tool of great leverage.

The uses for these extragalactic beacons are numerous. As test particles in the nearby Hubble flow, they have been used to measure the current expansion rate of the Universe (Sandage et al. 1992, 1994, 1996; Sandage & Tammann 1993; Schaefer 1994, 1995a,b, 1996; Branch & Tammann 1992; Tammann & Leibundgut 1990; Arnett, Branch, & Wheeler 1985; Cadonau, Sandage, & Tammann 1985; Hamuy et al. 1995; 1996a,b; Riess, Press, & Kirshner 1995a, 1996a; Riess et al. 1998a; Tripp 1998; Branch 1998 and references within). Combined with their positions on the sky, SNe Ia have been used to reveal the peculiar velocities of distant galaxies as well as the bulk flow of our own local neighborhood (Tammann & Leibundgut 1990; Miller & Branch 1992; Jerjen & Tammann 1993; Riess, Press, & Kirshner 1995b; Watkins & Feldman 1995; Riess et al. 1997b; Zehavi et al. 1998; Tammann 1998). SN Ia evolution is the only well understood time-variable process which can be used to mark the passage of time at high redshift. As cosmological clocks, SNe Ia have been used to examine the nature of the redshift using the time dilation test (Rust 1974; Leibundgut 1990; Goldhaber et al. 1997; Leibundgut et al. 1996; Riess et al. 1997a). SNe Ia have been employed as probes of extragalactic dust (Della Valle & Panagia 1993; Riess, Press, & Kirshner 1996b), and their contribution to galactic chemical enrichment by their production of iron peak elements has been explored by measuring their rates of occurrence (Timmes 1991; Cappellaro et al. 1993a,b, 1997; Turatto et al. 1994; van den Bergh & McClure 1994; Pain et al. 1997; Madau, Della Valle, & Panagia 1998). Recently, vigorous programs have embarked on searches for SNe Ia at high redshifts ($0.2 \leq z \leq 1.0$) with the intent of measuring the expansion history of the Universe (Perlmutter et al. 1995, 1997; Schmidt et al. 1998). Early results imply that there is not enough gravitating matter to close the Universe (Garnavich et al. 1998a; Perlmutter et al. 1998) and that currently the expansion is accelerating (Riess et al. 1998b; Perlmutter 1999). Supernova observations, when combined with measurements of Cosmic

Microwave Background anisotropies, may prove useful to determine the cosmic equation of state and the global geometry of the Universe (Garnavich et al. 1998b; White 1998).

These applications require well-observed SN Ia light curves with reliable photometry. Further, the cosmological applications rely on comparisons to nearby SNe Ia which delineate today’s Hubble flow ($0.01 < z < 0.1$).

Despite the importance of precisely observed SN Ia light curves, most published SN Ia photometry, before 1980, consisted of infrequently sampled photographic light curves for SNe within $cz < 2000 \text{ km s}^{-1}$ with a wide assortment of filters and emulsions (van den Bergh 1994; Cadonau & Leibundgut 1990; Barbon, Cappellaro, & Turatto 1989). Much of this data is plagued by systematic errors from non-linearities in detector sensitivity, uncertain transformations to modern filter conventions, and difficulties with background light subtraction. A crude estimate of these photometry errors comes from comparing the dispersion in Sandage & Tammann’s (1993) Hubble diagrams constructed with old photographic light curves (0.65 mag) with those based on more modern *B*-band SN Ia observations (0.38 mag; Hamuy et al. 1996a). The result suggests that typical errors from the pre-1980 photographic SN Ia photometry could be as high as ~ 0.5 magnitudes.

Obtaining well sampled light curves with high-precision photometry ($\sigma \leq 0.03 \text{ mag}$) is challenging. Collecting observations of SNe Ia in each of four filters every few days for ~ 100 days is a task that is not well suited to the short blocks of time allocated at most modern observatories. Variable weather poses another challenge to obtaining well-sampled SN Ia light curves. It is also important to maintain a telescope-detector setup throughout the observations which well matches standard passband conventions (Johnson & Harris 1954; Bessell 1990) since the non-stellar spectrum of an SN Ia can make linear color corrections inexact. The most challenging obstacle to producing a high-quality SN Ia light curve is to account correctly for the background light from the host galaxy *at the position of the supernova*.

Recent evidence has shown that SNe Ia are not perfectly homogeneous in luminosity or color and that the intrinsic luminosity and color is intimately related to the *shape* of the observed light curves (Phillips 1993; Riess, Press, & Kirshner 1995a, 1996a; Riess et al. 1998b; Hamuy et al. 1995, 1996a). Incorrectly subtracting the background light from a set of supernova observations can have disastrous

effects on the light curve shape. Boisseau & Wheeler (1991) have investigated the effect of background galaxy contamination on the inferred absolute magnitude and light-curve speed of SNe Ia. They find that oversubtraction or undersubtraction of a constant flux source leads to an observed correlation between SN Ia light curve speed and inferred luminosity. If the value of this correlation were the same as the intrinsic correlation, then using the light-curve shape to correct the luminosity could equally well account for either intrinsic luminosity variation or galaxy contamination. Unfortunately, they are not the same, so it is crucial to account correctly for the background light to determine the true light-curve shape. SN Ia light curves obtained by the Calán/Tololo survey show that with high quality photometry, it is possible to measure distances with SN Ia light curves to a precision approaching $\sim 5\%$ (Hamuy et al. 1995, 1996a; Riess, Press & Kirshner 1995a, 1996a).

Since the widespread use of modern CCD detectors coupled with commercially available Johnson/Cousins passbands began in ~ 1980 , there have been nearly 250 SNe Ia reported (van den Bergh 1994; Barbon, Cappellaro, & Turatto 1989). Regrettably, light curves have been collected, reduced, and published for fewer than 50 of these objects (Cadonau & Leibundgut 1990; Hamuy et al. 1993; Hamuy et al. 1994; 1996b; Sadakane et al. 1996; Phillips 1993 and references within). Of these, less than half include *I* and *R* light curves which, combined with shorter wavelength light curves, can be used to determine the reddening due to dust (Ford et al. 1993; Hamuy et al. 1996b).

Recently, progress has been made toward building a reliable sample of SN Ia light curves in the Hubble flow. The largest contribution to date has been made by the Calán/Tololo Supernova Survey, a program begun in 1990 by astronomers at Cerro Tololo Inter-American Observatory (CTIO) and the Cerro Calán Observatory of the University of Chile (Hamuy et al. 1993). This photographic search with follow-up *B,V,I* CCD photometry netted 27 SNe Ia with $(0.01 < z < 0.1)$. Other programs which show great promise include the Beijing Astronomical Observatory search (IAUC 6379), the Mount Stromlo Abell Cluster Supernova Search (Reiss et al. 1998), and the Lick Observatory Supernova Search (IAUC 6627), all of which have made repeated discoveries and in the future are expected to contribute to the growing sample of SN Ia light curves.

Beginning in 1993, astronomers at the Center for Astrophysics (CfA) began a concerted and organized

effort to collect Johnson/Cousins *BVRI* photometry of type Ia supernovae. Many of these SNe Ia were discovered serendipitously by amateurs or by professionals scanning images collected for another purpose. This work presents the light curves of 22 of SNe Ia in the Hubble flow observed between 1993 and 1996. In §2 we give details of our observational setup and reduction procedure. We present *BVRI* photometry for 22 SNe Ia in §3. In §4 we discuss the characteristics of this sample.

2. Observations & Reductions

Most of the photometric data presented in this paper were collected at the 1.2 m telescope at the Fred Lawrence Whipple Observatory (FLWO). The 1.2 m is an $f/8$ Ritchey-Chretien reflector and was outfitted with a thick front-illuminated Loral CCD between 1993 and July 1995, and a thinned, back-side illuminated Loral CCD from August 1995 through 1996. The surfaces of both CCDs were coated with a laser dye which improves the blue sensitivity. The pixels are 15 microns square, corresponding to 0.31 arcseconds at the focal plane of the 1.2 m telescope. The filters are constructed from Schott glass components recommended by Bessell (1990) for a coated CCD.

The B , V , R , and I CCD transmission functions for the FLWO 1.2 m telescope are shown in Figure 1 (Andy Szentgyorgyi, private communication). The CCD's ability to detect light over a range of wavelengths makes it difficult to emulate the sharp blue-side or red-side cut-offs of photomultiplier transmission functions. The B and V CCD transmissions closely match the photomultiplier passband conventions of Johnson & Harris (1954) and most recently Bessell (1990). The R -band CCD transmission is similar to Cousins (1980, 1981) and Bessell (1990). The I -band CCD transmission extends to substantially longer wavelengths than the Cousins (1980, 1981) and Bessell (1990) convention for the I photomultiplier passband. The FLWO CCD transmissions are very similar to CCD transmission functions obtained by Bessell with the filters he prescribed (Bessell 1990). We use linear color corrections to account for differences between our CCD transmission functions and the Johnson/Cousins photomultiplier passbands. Still, broad emission and absorption features in the spectral energy distribution of SN Ia can cause variations among light curves observed with slightly different CCD transmission functions. The difference between broad-band SN Ia photometry obtained at FLWO and CTIO has been determined in detail by Smith et al. (1998) by comparing phototmetry of SN 1994D obtained at the two sites. These differences (with uncertainties in

parenthesis), as shown in Table 1, are small, but not entirely absent. Agreement between FLWO and CTIO is best in the V passband.

A small number of the observations reported here were conducted at the 0.62 m telescope at the Capilla Peak Observatory (CPO). The 0.62 m is a $f/15.2$ Boller & Chivens Cassegrain telescope matched with a RCA model SID501EX back-illuminated and thinned CCD. The CCD pixels are 30 microns square, corresponding to 0.67 arcseconds per pixel at prime focus. The CPO CCD transmission functions are shown by Beckert & Newberry (1989) and are a good match to the CCD transmissions at FLWO. The mean difference in SN Ia photometry obtained at FLWO and CPO is shown in Table 1 using SN 1995D. The difference is very small in V and somewhat larger in B , R , and I . Approximately 10 of the more than 1200 photometric observations were collected at other observatories including the Michigan-Dartmouth-MIT Observatory, the McDonald Observatory, the McGraw Hill Observatory, the Lick Observatory, and CTIO as noted in the photometry tables.

A well-sampled SN Ia light curve requires monitoring every day or two near maximum light and every few days as it changes more slowly a fortnight after maximum. Weather and moonlight often intercede even when an observatory is well-organized and well-instrumented to gather these observations. Fortunately, photometric weather is not required since we can use stars in the SN field as local calibrators to monitor the changing brightness of the SN Ia through differential photometry. Optimal comparison stars are the brightest stars in the field which do not saturate the CCD electron wells during the long SN Ia exposures at late times when the supernova has dimmed. Comparison stars obviate the need to make first-order airmass corrections and allow the SN Ia brightness to be measured in any weather conditions for which the supernova is visible.

On nights which are photometric, we performed all-sky photometry from which we constructed a transformation from our detector measurements to the standard photometric conventions. Following Hardie (1962) and Harris et al. (1981), we used transformation equations which gave the apparent magnitude as a linear combination of the instrumental magnitude, observed airmass, and color. Using all-sky standard stars from Landolt (1992) we then solved for the linear coefficients of the transformation equations. The typical rms scatter of our transformations was 0.02 mag, with no observed correlation between residuals

and color, airmass, or instrumental magnitude. The mean color terms for the FLWO 1.2 m were 0.04, -0.03, -0.08, and 0.06 mag in B , V , R , and I per mag of $B - V$, $B - V$, $V - R$, and $V - I$, respectively. These transformations were employed to calibrate the apparent magnitudes of the comparison stars which were observed on the same night as the Landolt standards.

The comparison stars used for each SN Ia field are marked in Figure 2 and their B , V , R , and I apparent magnitudes are given in Table 2. For two fields (as listed in Table 2), only one “primary” comparison star was consistently visible in the field of view.

For each night a SN Ia was observed, we measured the brightness of the supernova relative to one or more comparison stars in the field. Extreme care was exercised to subtract properly the background light at the location of the supernova. For SNe Ia far from the galaxy, or on a smooth and uniform region of the galaxy, reliable background subtraction was easily accomplished. In such cases, we generally measured the background light from the median sky value contained in an annulus of width $\sim 6''$ at an inner distance of $\sim 8''$ from the center of the supernova. These separations were increased as needed for data from nights with poor seeing. More challenging were SNe Ia located on a luminous and mottled galaxy background. In this case, unless images of the galaxy existed prior to explosion, the only reliable way to proceed was to wait for the SN Ia to fade away to obtain an image of the galaxy without the supernova. Then by carefully matching the alignment, intensity, and point-spread functions of the images with and without the SN Ia present, we subtracted the two images to obtain an image of the supernova with zero background (Schmidt et al. 1998). This is the same method used for the photometry of high-redshift SNe Ia (Riess et al. 1998b).

To measure the brightness of the supernova relative to the comparison stars in an uncrowded field we used the method of aperture photometry. We added the light contained in a series of apertures of increasing radius around the star and supernova and found the difference in magnitude between the SN Ia and the comparison star which was independent of aperture radius. The estimated background was varied until a difference in magnitude was found which was independent of aperture radius. This procedure is refined for crowded fields or faint SNe Ia where we have fit point spread functions (PSFs) to the SN Ia and comparison stars to determine their relative brightness. Experience has shown that when either technique is suitable, the aperture method and the PSF method give consistent results within 0.01 mag. The particular method

used to derived the photometric measurements for each SN is listed in Table 3.

3. SN Ia Data

B , V , R , and I band photometry for 22 SN Ia light curves is given in Tables 6 through 27 and plotted in Figure 3. For each observation we include an estimate of the 1σ error which was determined from Poisson statistics, image quality, and uncertainty in the calibration of the comparison stars. In most cases the dominant source of uncertainty is the comparison star calibration. In Table 3 we give details relevant to the SN Ia observations including heliocentric redshift (column 2), the peak of the B light curve (column 2), the peak of the V light curve (column 3), the decline in B 15 days after maximum, $\Delta_{m15}(B)$ (column 4), time of the first observation relative to B maximum (column 5) as determined by the multicolor light curve shape (MLCS) fit, right ascension (column 6), declination (column 7), and the photometric reduction technique (column 8) used to measure the SN Ia’s brightness. The redshifts for SNe 1994S, 1994ae, 1995D, 1995E, 1995al, 1996Z, 1996ai, 1996bo, 1996bk, and 1996bv are from Huchtmeier & Richter (1989); SN 1993ae is from Chincarini & Rood (1977); SN 1995ak is from IAUC 6254; SN 1996bo is from IAUC 6492; and SN 1996X is from the RC3 catalogue (de Vaucouleurs et al 1991). The rest were determined from our spectra of the host galaxies.

The peaks of the B and V light curves and values of $\Delta_{m15}(B)$ were determined from a light curve fitting method which was *different* from that employed by Hamuy et al. (1996b). These values should not be compared directly to the values given by Hamuy et al. (1996b). The only consistent way to combine the parameters of the SNe Ia here and in Hamuy et al. (1996b) is to fit all of these data with a single fitting method.

Table 4 lists information relevant to the host galaxies of the CfA SN Ia sample. This includes the galaxy designation (column 2), the morphological type (column 3), the $B - V$ color of the host galaxy, and the offset between the galaxy center and the SN Ia. The offsets were determined from a flux weighted centroid for the SN and the galaxy in V . The $B - V$ galaxy colors were determined from the largest apertures (typically $\sim 20''$) which avoided any foreground point source contamination. The same size aperture was used to measure the galaxies magnitudes in B and V . The measured galaxy colors have an

uncertainty of $\sigma = 0.1$ mag.

Table 5 contains information relevant to the discovery and identification of each SN Ia. This includes the discoverer and IAUC announcement (column 2), the method of image recording (column 3), the date of discovery (column 4), and the observers who provided the spectral classification of the supernova (column 5). We have obtained spectra of each of these SNe Ia from the FLWO and after thorough examination we have found that each was of type Ia as defined by Branch, Fisher, & Nugent (1993) and Filippenko (1997). Two objects, SN 1995ac and SN 1995bd, displayed similar spectral characteristics as the peculiar SN Ia 1991T including strong Fe III and weak Si II absorption (Garnavich et al. 1996).

4. Discussion

Many of these SNe Ia have been previously utilized for a variety of cosmological measurements as discussed in §1. Nearly all of these applications make use of estimates of the luminosity distances to these SNe Ia. The discussion of the most precise way to infer these distances has evolved from the assumption of homogeneity (Leibundgut 1988; Branch & Miller 1993; Sandage & Tammann 1995) to methods which account for the correlation between light-curve shape and luminosity (Riess, Press, & Kirshner 1995a; Hamuy et al. 1995, 1996a) and employ multiple passbands to separate the effects of dust on SN Ia light from those of luminosity (Riess, Press, & Kirshner 1996a; Riess et al. 1998b). These methods are continually evolving and improving and the specific values of the distance related parameters will likely be superseded regularly. For this reason, we explore characteristics of this sample which are largely independent of the SN distances.

In Figure 4 we show histograms of the supernova redshifts, peak apparent magnitude, epoch of first observation, number of observations, absolute magnitude determined from the luminosity/light-curve parameter, and line-of-sight extinction. For comparison we include the same statistics for the 27 SNe Ia from the Calán/Tololo Supernova Survey (C/T). The CfA sample has a redshift range of $0.003 < z < 0.124$ with a mean redshift of $z = 0.025$. As seen in Figure 4, the redshifts are concentrated at lower values, though most are within the Hubble flow: in the rest frame of the cosmic microwave background (CMB), 17 of the 22 SNe Ia have $cz > 2500 \text{ km s}^{-1}$. For the C/T sample the redshift range is $0.011 < z < 0.101$ with

a mean of $z = 0.045$.

The following sample characteristics are derived from multi-color light curve shape (MLCS) fits to the *BVRI* data as described by Riess, Press, & Kirshner (1996a) and reanalyzed by Riess et al. (1998a); they are subject to future refinements of fitting methods. The fitted peak apparent magnitudes for the CfA sample range from $13.16 < m_V < 19.52$ with a mean of $m_V = 15.70 \pm 1.65$. For the C/T sample the range is $14.64 < m_V < 19.35$ with a mean of $m_V = 17.24 \pm 1.30$. The epoch of the first light curve observation for the CfA sample ranges from 12 days before maximum to 10 days after maximum. The average starting epoch is coincident with B maximum with half of the SNe beginning before this time. The C/T sample ranges between 10 days before to 12 days after maximum with a third beginning before maximum. Figure 4 shows a histogram of the absolute magnitudes as inferred from the MLCS light-curve shape fits on the Cepheid distance scale (Riess, Press, & Kirshner 1996a). The range of luminosities implied for the CfA sample is $-19.87 < M_V < -18.80$ with a mean of $M_V = -19.40 \pm 0.28$; the C/T sample has $-19.68 < M_V < -18.81$ with a mean of $M_V = -19.27 \pm 0.29$. A true SN Ia luminosity function can only be derived from a sample of SNe Ia with well understood selection criteria (Reiss et al. 1998). Figure 4 also shows the distribution of visual band extinctions as inferred from the MLCS measurements of reddening. This distribution is strongly peaked toward low extinctions, with three notable exceptions (SN 1995E, SN 1995bd, and SN 1996ai) each having more than one visual magnitude of obscuration. One of these, SN 1995bd, is expected to have 1.5 mag of visual extinction from the Milky Way Galaxy (Schlegel, Finkbeiner, & Davis 1998). Four more objects (SNe 1993ac, 1996bv, 1996bo, and 1996bk) have 0.5-1.5 mag of visual extinction.

While the completeness and biases of the CfA SN Ia sample are not easily defined, it is still interesting to combine these supernovae with the C/T sample to look for patterns in a large data set. Figure 5 shows the extinction and light-curve shape parameters as a function of supernova galactocentric distance and host galaxy type. Host galaxy extinction decays rapidly with projected separation from the nucleus and with the progression to earlier type galaxies. The multicolor light-curve shape parameter (Riess, Press, & Kirshner 1996a) shows that slow decline rates ($\Delta < 0$) dominate at small galactocentric distances and that there is a general trend, first pointed out by Hamuy et al. (1996), for faster decline rates for supernovae

occurring in early-type galaxies. Figure 6 shows the distribution of absolute magnitude for SNe Ia in the Hubble flow versus projected separation from the host galaxy. When no correction is made for extinction or light-curve shape, the luminosity variation is similar to that found by Wang, Höflich, & Wheeler (1997); there is a large dispersion at small galactocentric distances which decreases outward. However, when the luminosity is corrected for total extinction (Figure 6b) from MLCS, SNe with projected separations of less than 10 kpc are found, on average, to be brighter by about 0.3 mag than those further out. Because the projected separation is the minimum distance the supernova can be from the galaxy center, the few faint objects at small projected separations could be at even larger galactocentric distances. Elliptical hosts dominate the sample at large separations, so the decrease of SN Ia luminosity in early-type hosts found by Hamuy et al. (1996a) may contribute to this trend. When the luminosity is corrected for both extinction and light-curve shape, no trend with galactocentric distance is apparent.

A Hubble diagram of the 17 SNe Ia from the CfA sample with $cz > 2500 \text{ km s}^{-1}$ is given in Figure 7. These distances were derived with the MLCS method (Riess, Press, & Kirshner 1996a) as prescribed by Riess et al. (1998b) in B, V, R , and I . The dispersion of these distances is $\sigma = 0.16 \text{ mag}$. As noted by Zehavi et al. (1998), the SNe Ia within $cz \approx 7000 \text{ km s}^{-1}$ ($\log cz \approx 3.85$) exhibit the dynamic complement of a local void: an increased expansion rate relative to the more distant SNe Ia (see also Tammann 1998). For these SNe Ia, the difference between the expansion rates within and beyond $\sim 7000 \text{ km s}^{-1}$ is 7%. It is interesting to note that the sense of this change in the expansion rate is opposite to what would be caused by a selection bias that emphasizes more luminous supernovae at larger distances. The observed effect corresponds to a higher Hubble constant inferred locally. If a more statistically significant sample of SNe Ia upholds this hint of a local void, it would help explain why SNe Ia yield a lower Hubble constant than distance indicators that refer to more local volumes (Freedman et al. 1998; Jacoby et al. 1992).

The 22 $BVRI$ SN Ia light curves presented here are composed of 1210 individual observations, and comprise some of the most highly sampled illustrations of the photometric history of SNe Ia in the Hubble flow. A histogram of the number of observations for each SN Ia is shown in Figure 4. Standouts include SNe 1994ae, 1995D, 1995al, 1995bd, 1995ac, and 1996X, each with 80 to 100 observations beginning before maximum and extending 60 to 100 days after maximum. Figure 8 shows $BVRI$ composite light curves

formed by normalizing the data in time and brightness at the fit to the initial peak, including a correction for $1 + z$ time dilation and a K -correction (Hamuy et al. 1993). By affixing the light curves at maximum, their inhomogeneity is readily apparent. For example, in B the light curves exhibit a decline in B 15 days after maximum [$\Delta m_{15}(B)$] of $0.85 < \Delta m_{15}(B) < 1.55$ mag and in I the time and brightness of the second maximum exhibits considerable variations. These and other features of the light curves have been shown to correlate with the luminosity and colors of SNe Ia (Phillips 1993; Riess, Press, & Kirshner 1995a, 1996a; Hamuy et al. 1995, 1996a,b). It is this property of SNe Ia which has recently enhanced their precision as distance indicators and may lead to a better understanding of their progenitors and physical structure (Höflich, Wheeler & Thielemann 1998).

We are deeply indebted to numerous observers on the 1.2 meter at Mt. Hopkins who graciously observed our supernovae and enabled us to construct light curves of unprecedented sampling. We also wish to thank Paul Schechter and Denise Hurley who contributed to the compilation of these data. The work at U.C. Berkeley was supported by the Miller Institute for Basic Research in Science as well as NSF grant AST-9417213, Supernova research at Harvard is supported by the NSF through grants AST-9528899 and AST-9218475.

References

- Arnett, W.D., Branch, D., & Wheeler, J.C. 1985, Nature 314, 337
- Barbon, R., Cappellaro, E., & Turatto, M. 1989, A&AS, 81, 421
- Beckert D.C. & Newberry, M.V. 1989, PASP, 101, 849
- Bessell, M.S. 1990, PASP, 102, 1181
- Boisseau, J.R., & Wheeler, J.C. 1991, AJ, 101, 1281
- Branch, D. 1998, ARAA, in press
- Branch, D., & Miller, D. 1993, ApJ, 405, L5
- Branch, D. & Tammann, G.A. 1992, ARA&A, 30, 359
- Branch, D., Fisher, A., & Nugent, P. 1993, AJ, 106, 2383
- Cadonau, R., Sandage, A., & Tammann, G.A. 1984, Lecture Notes in Physics, V224, 151
- Cadonau, R., & Leibundgut, B. 1990, A&AS, 82, 145
- Cappellaro, E., Turatto M., Bennetti, S., Tsvetkov, D. Yu., Bartunov, O. S., & Makarova, I. J. 1993a, A&A, 268, 472
- Cappellaro, E., Turatto M., Bennetti, S., Tsvetkov, D. Yu., Bartunov, O. S., & Makarova, I. J. 1993b, A&A, 283, 383
- Cappellaro, E. et al. 1997, A&A, 322, 431
- Chincarini, G., & Rood, H. 1977, ApJ, 214, 351
- Cousins, A. W. J. 1980, S. Afr. Astron. Obs. Circ, 1, 166
- Cousins, A. W. J. 1981, S. Afr. Astron. Obs. Circ, 6, 4
- de Vaucouleurs, G. et al. 1991, in *Third Reference Catalogue of Bright Galaxies* (Springer-Verlag, New York)
- Della Valle, M., & Panagia, N. 1992, AJ, 104, 696
- Ford, C. et al. 1993, AJ, 106, 3
- Freedman, W. et al. 1998, astro-ph/9801080
- Garnavich, P. M., et al. 1998a, ApJ, 493, 53
- Garnavich, P. M., et al. 1998b, ApJ, in press

- Garnavich, P. M., et al. 1996, AAS, 189, 4509
- Goldhaber, G., et al., 1997, in *Thermonuclear Supernovae*, ed. P. Ruiz-Lapuente, R. Canal, & J. Isern, Dordrecht: Kluwer, p. 777
- Hamuy, M., Phillips, M. M., Suntzeff, N. B., Schommer, R. A., Maza, J., & Avilés, R. 1996a, AJ, 112, 2398
- Hamuy, M., et al. 1996b, AJ, 112, 2408
- Hamuy, M., Phillips, M. M., Maza, J., Suntzeff, N. B., Schommer, R. A., & Aviles, A. 1995, AJ, 109, 1
- Hamuy, M., Phillips, M. M., Maza, J., Suntzeff, N. B., Schommer, R. A., & Aviles, A. 1994, AJ, 108, 2226
- Hamuy, M., et al. 1993, AJ, 106, 2392
- Hardie, R. H., 1962, in *Stars and Stellar Systems, Vol. 2, Astronomical Techniques*, ed. W.A. Hiltner, (Chicago: University of Chicago Press), p. 198
- Harris, W. E., Fitzgerald, M. P., & Reed, B. C. 1981, PASP, 93, 507
- Hatano, K., Branch, D., & Deaton, J. 1998, ApJ, 502, 177
- Höflich, P., Wheeler, J. C., & Thielemann, F. K. 1998, ApJ, 495, 617
- Huchtmeier, W., & Richter, G., 1989, in *A General Catalog of HI Observations of Galaxies*, (Berlin: Springer)
- Jacoby, G. H., et al. 1992, PASP, 104, 599
- Johnson, H. L., & Harris, D. L., 1954, ApJ, 120, 196
- Jerjen, H., & Tammann, G.A. 1993, A&A, 276, 1
- Landolt, A.U. 1992, AJ, 104, 340
- Leibundgut, B. et al. 1996, ApJ, 466, L21
- Leibundgut, B. 1990, A&A, 229, 1
- Madau, P., Della Valle, M., & Panagia, N., 1998, MNRAS, 297, 17
- Maza, J., Hamuy, M., Phillips, M., Suntzeff, N., & Aviles, R. 1994, ApJ, 424, L107
- Nugent, P., Phillips, M., Baron, E., Branch, D., & Hauschildt, P., 1995, ApJ, 455, L147
- Pain, R. et al., 1997, in *Thermonuclear Supernovae*, ed. P. Ruiz-Lapuente, R. Canal, & J. Isern, Dordrecht: Kluwer, p. 790
- Perlmutter, S., et al., 1998, Nature, 391, 51
- Perlmutter, S., et al., 1997, ApJ, 483, 565

- Perlmutter, S. et al., 1995, ApJ, 440, 41
- Phillips, M. 1993, ApJ, L105
- Riess, A. G., Nugent, P. E., Filippenko, A. V., Kirshner, R. P., & Perlmutter, S., 1998a, ApJ, 504, 935
- Riess, A. G. et al., 1998b, AJ, 116, 1009
- Riess, A. G., et al. 1997a, AJ, 114, 722
- Riess, A. G., Davis, M., Baker, J., & Kirshner, R. P. 1997b, ApJ, 488, L1
- Riess, A. G., Press W. H., & Kirshner, R. P. 1996a, ApJ, 473, 88
- Riess, A. G., Press W. H., & Kirshner, R. P. 1996b, ApJ, 473, 588
- Riess, A. G., Press W. H., & Kirshner, R. P. 1995a, ApJ, 438, L17
- Riess, A. G., Press W. H., & Kirshner, R. P. 1995b, ApJ, 445, L91
- Rust, B.W., PhD Thesis, Oak Ridge National Laboratory (ORNL-4953)
- Sadakane, K. et al., 1996, PASJ, 48, 51
- Saha, A. et al., 1994, ApJ, 425, 14
- Sandage, A. et al. 1996, ApJ, 460, L15
- Sandage, A. et al. 1994, ApJ, 423, L13
- Sandage, A., & Tammann, G. A., 1993, ApJ, 415, 1
- Sandage, A., Tammann, G. A., Panagia, N., & Macchetto, D. 1992, ApJ, 401, L7
- Schaefer, B. E., 1996, ApJ, 464, 404
- Schaefer, B. E., 1995a, ApJ, 447, L13
- Schaefer, B. E., 1995b, ApJ, 449, L9
- Schaefer, B. E., 1994, ApJ, 426, 493
- Schlegel, D. J., Finkbeiner, D. P., & Davis, M. 1998, ApJ, 500, 525
- Schmidt, B. P., et al. 1998, ApJ, in press
- Shaw, R. L. 1979, A&A, 76, 188
- Smith, C. et al. 1998, in preparation
- Strauss, M. A., & Willick, J. A. 1995, PhR, 261, 271
- Tammann, G. A., 1998, astro-ph/9805013
- Tammann, G. A., & Sandage, A. 1995, ApJ, 452, 16

- Tammann, G. A., & Leibundgut, B. 1990, A&A, 236, 9
- Timmes, F. X., 1991, in *Supernovae*, ed S.E. Woosley, Springer Verlag, New York
- Tripp, R., A&A, 1998, 331, 815
- Turatto, M., Cappellaro, E., & Benetti, S. 1994, AJ, 108, 202
- van den Bergh, S., & McClure, R. D. 1994, ApJ, 425, 205
- van den Bergh, S. 1994, ApJS, 92, 219
- Vaughan, T. E., Branch, D., Miller, D.L., & Perlmutter, S. 1995, ApJ, 439, 558
- Wang, L., Höflich, P., & Wheeler, J. C. 1997, ApJ, 483, L29
- Watkins, R., & Feldman, H. A. 1995, ApJ, 453, L73
- White, M. 1998, astro-ph/9802295

Figure 1: The solid and dotted lines show the B , V , R , and I CCD transmission functions for the FLWO 1.2 m telescope as determined from the FLWO passband filters and the quantum efficiency curve of the FLWO thick and thin CCD, respectively. These are compared to the Bessell (1990) representation of the Johnson/Cousins convention for the B , V , R , and I phototube transmissions (dashed line). The sharp phototube transmission functions of the Johnson/Cousins convention are not perfectly matched using CCD detectors which are sensitive to light over a range of wavelengths.

Figure 2: Photometry comparison stars in the fields of 22 SNe Ia. The stars used for measuring the brightness of each SN Ia are listed in Table 2 and indicated in the figures. The orientation of each field is North at the top and East to the left. The horizontal arrow at the top left indicates the length of one arcminute.

Figure 3: B , V , R , and I light curves of 22 SNe Ia. The V light curves (filled circles) are plotted without an offset. The B light curves (open circles) are plotted at $\sim +1$ mag offset from V , the R light curves (open diamonds) are plotted at ~ -1 mag offset from V , and the I light curves (open squares) are plotted at ~ -2 mag offset from V . The lines are the MLCS empirical fits to the data (Riess, Press, & Kirshner 1996a; Riess et al. 1998b).

Figure 4: Characteristics of CfA SN Ia sample. Shown with solid lines are histograms of the redshifts (z), apparent magnitude (m_V), epoch of first V observation relative to B maximum, number of observations, absolute magnitude (M_V) as determined from the luminosity/light-curve parameter, and line-of-sight visual extinction, A_V . The last three parameters are derived from MLCS empirical fits to the data (Riess, Press, & Kirshner 1996a; Riess et al. 1998b). Shown in dash-dot lines are the same characteristics for the Calán/Tololo Supernova Survey (C/T).

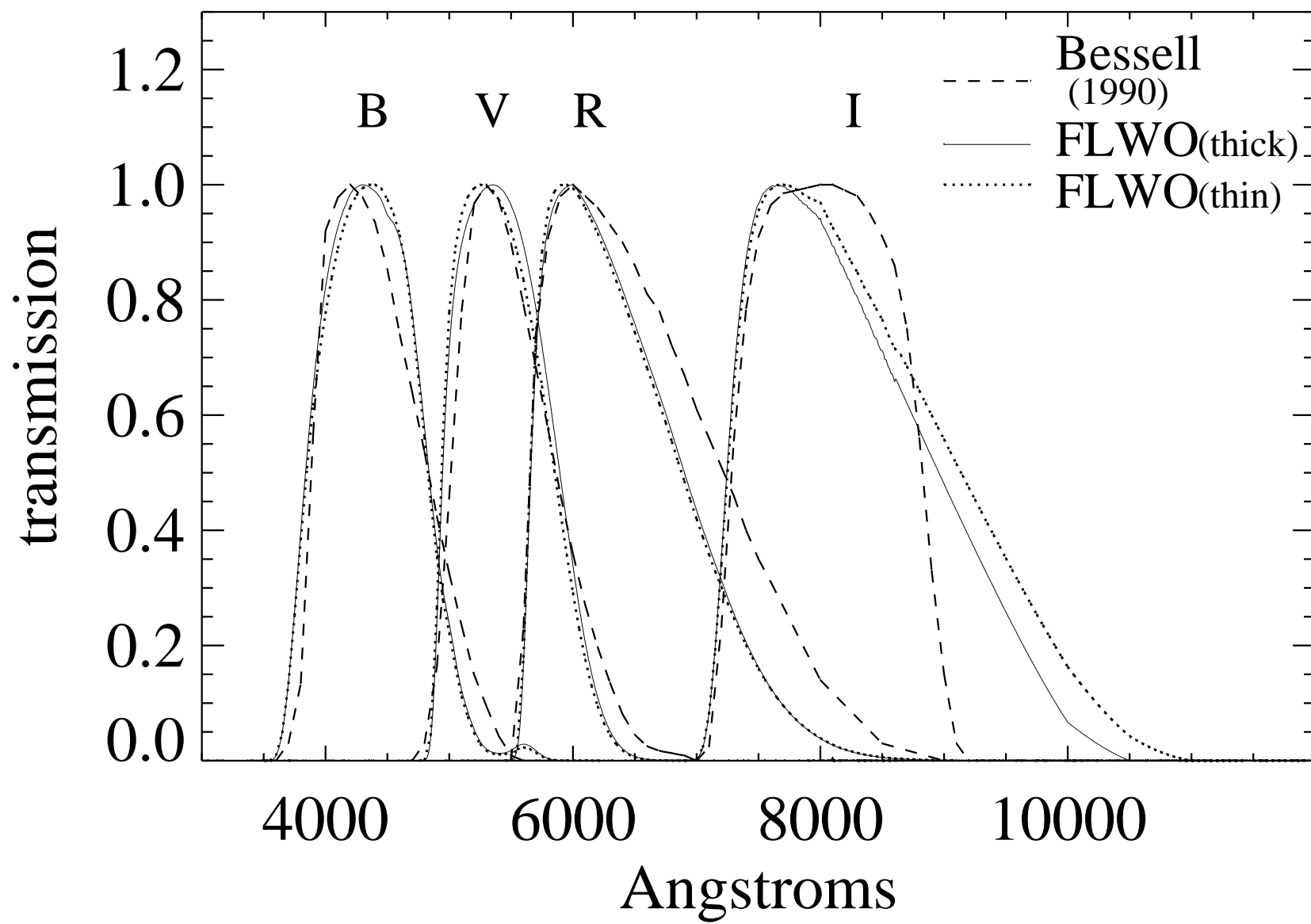
Figure 5: SN Ia extinction and light curve parameter trends with galactocentric distance and host galaxy morphology. A general decrease of host galaxy extinction is seen with galactocentric distance and an increase with the lateness of host galaxy type. A weak trend of the MLCS light-curve parameter, Δ , is that SNe Ia with comparatively faster (dimmer) light curves occur further from the center of galaxies and are more common to early-type galaxies. The CfA SNe Ia are shown as filled symbols, the C/T SNe Ia are shown as open symbols, and SNe Ia calibrated by Cepheid variables are shown as X's.

Figure 6: SN Ia luminosity versus galactocentric distance. The luminosities of SNe Ia, uncorrected

for light-curve shape or extinction (a), display a greater variation closer to the galaxy centers as noted by Wang, Höflich, & Wheeler (1997). After correction for extinction (b), SNe Ia with projected separations of less than 10 kpc are, on average, brighter by about 0.3 mag than those further out. This relation is also shown by host galaxy type (d). After the luminosities are corrected for light-curve shape and extinction, no significant trend with galactocentric distance is apparent (c). The CfA SNe Ia are shown as filled symbols, the C/T SNe Ia are shown as open symbols.

Figure 7: Hubble diagram of CfA sample 17 SNe Ia with $cz > 2500 \text{ km s}^{-1}$. The distances are determined by empirical MLCS fits to the light curves described by Riess, Press, & Kirshner (1996a), and updated by Riess et al. (1998b).

Figure 8: Composite B , V , R , and I SN Ia light curves. These light curves were made by normalizing the 22 CfA SN Ia sample light curves in time and brightness at the fit to the initial peak, including a correction for $1 + z$ time dilation and a K -correction. They include over 1200 individual data points. The inhomogeneity of the light curves is readily apparent.

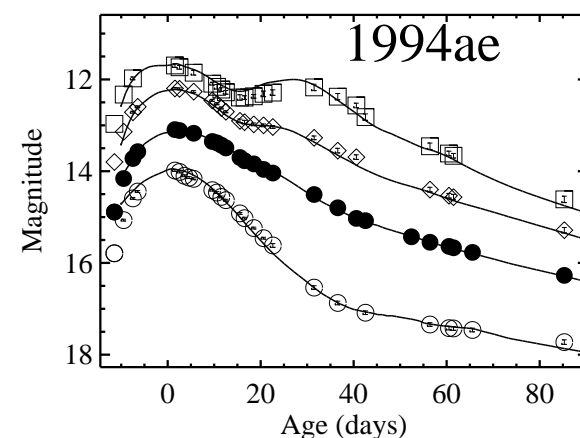
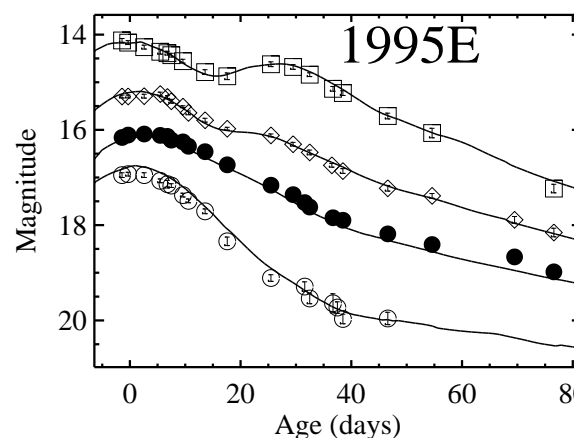
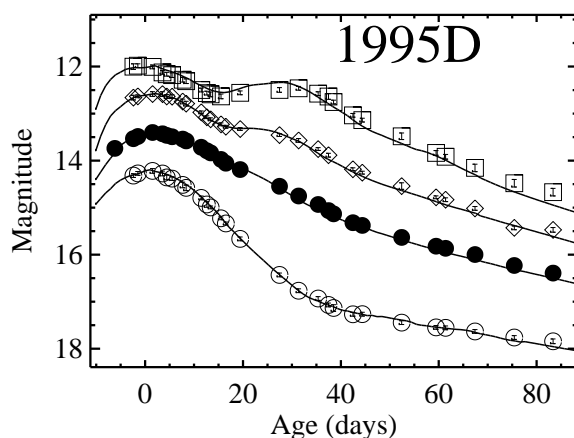
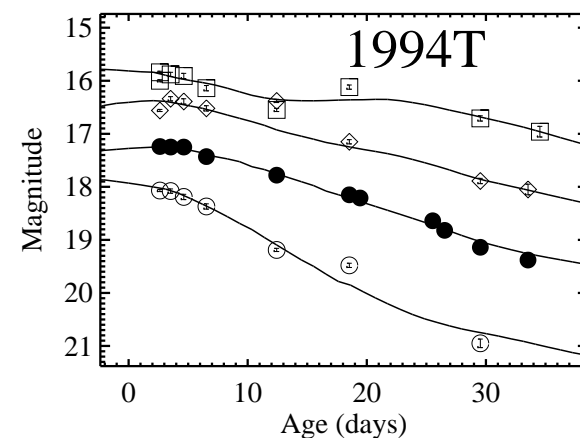
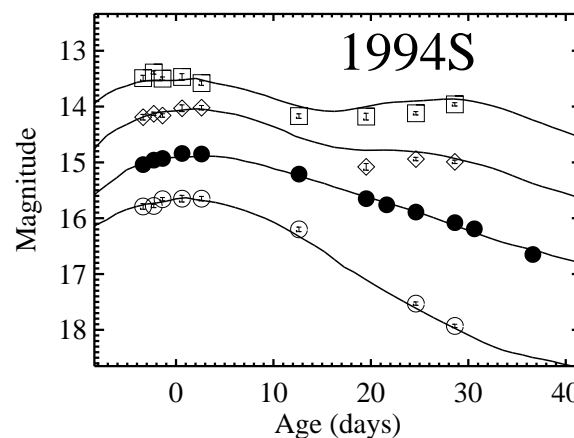
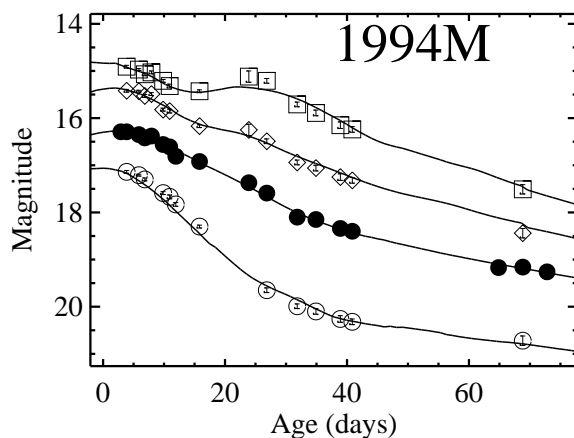
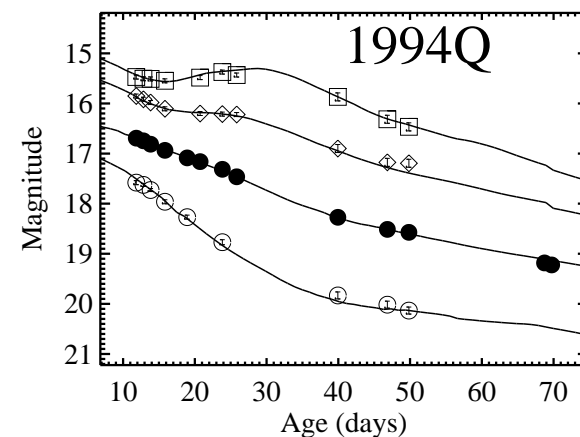
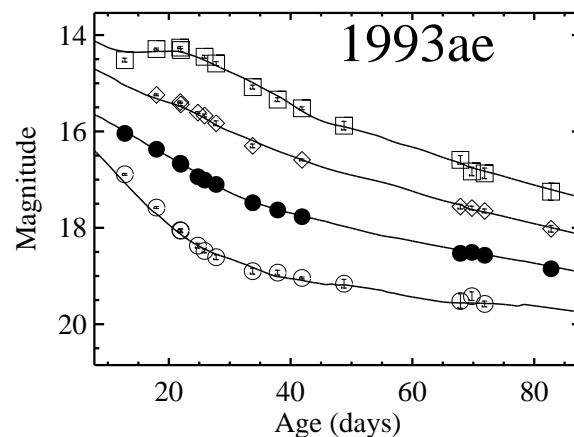
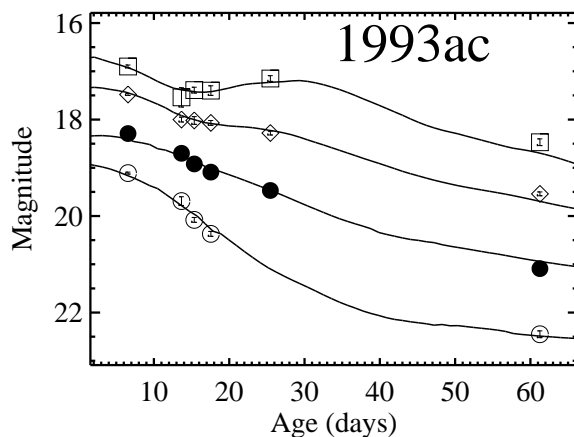


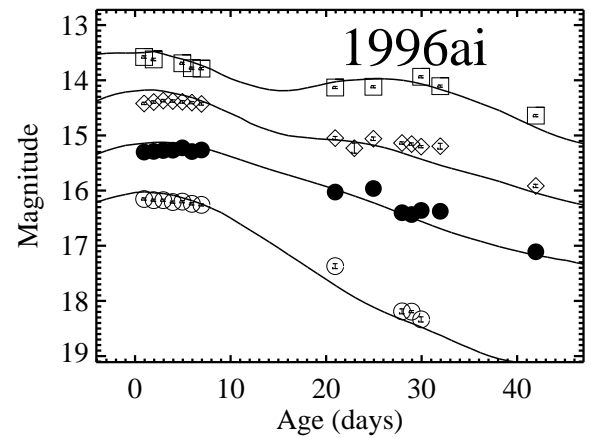
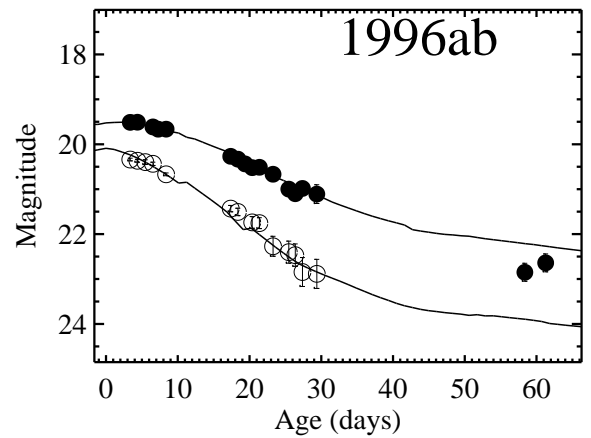
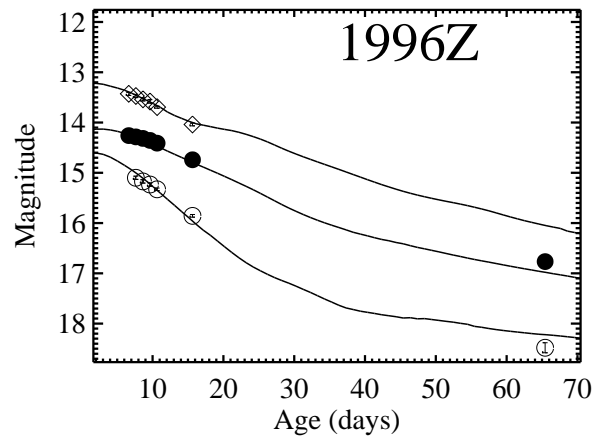
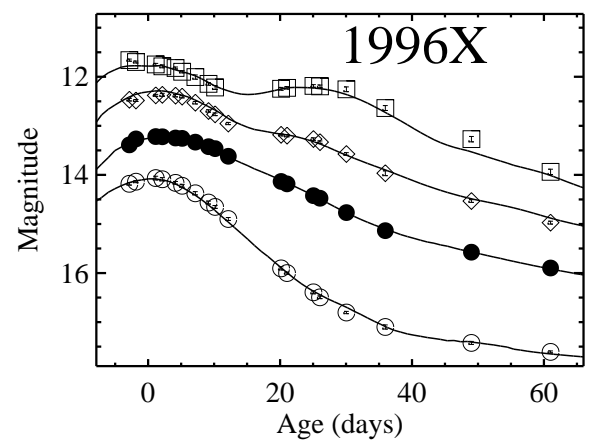
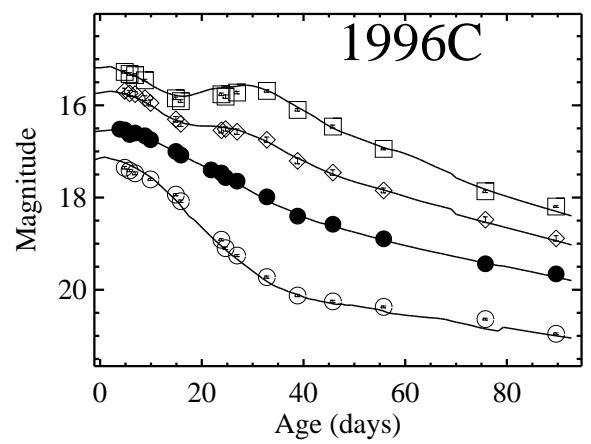
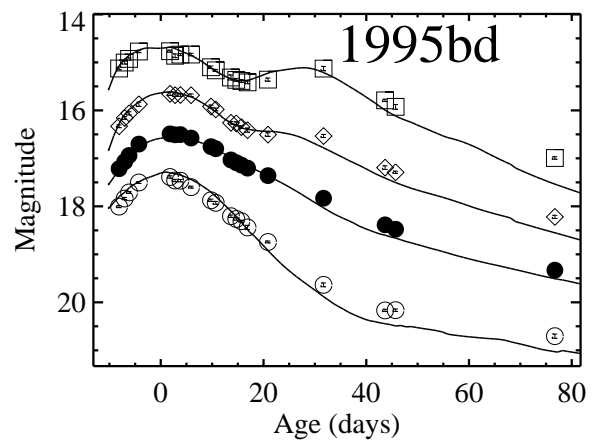
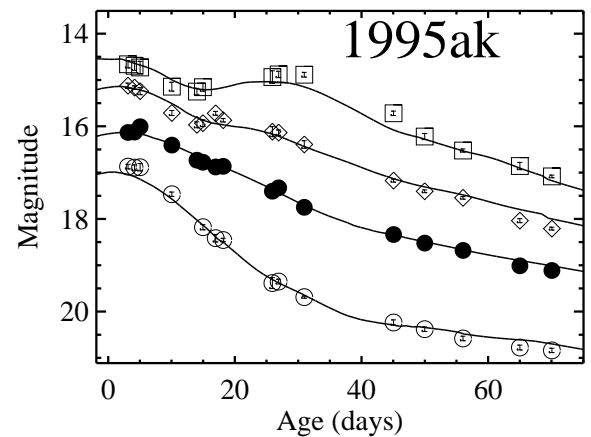
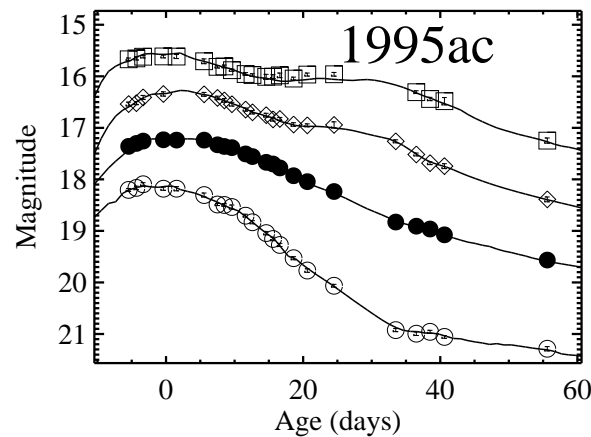
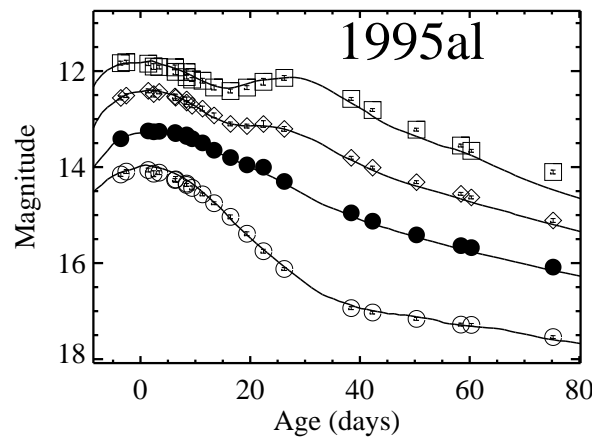
This figure "ariess.fig2.1.gif" is available in "gif" format from:

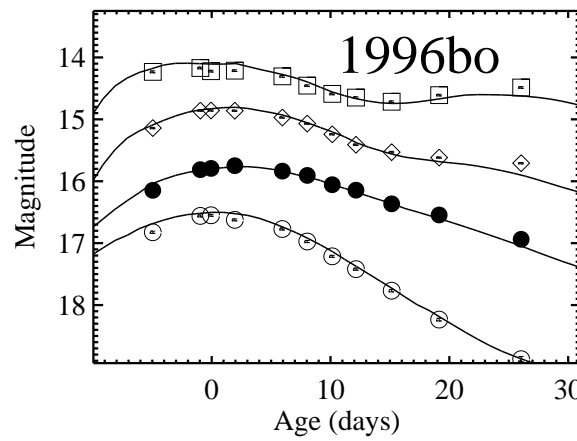
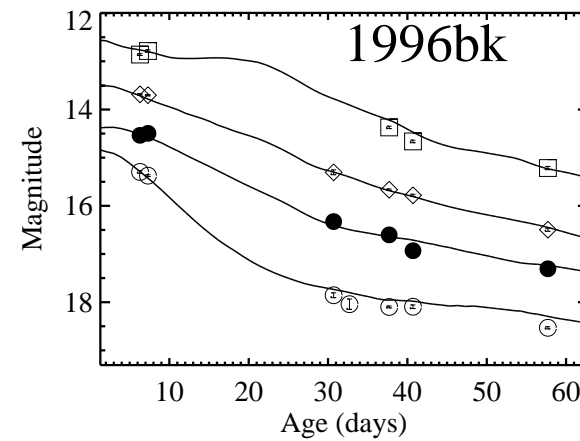
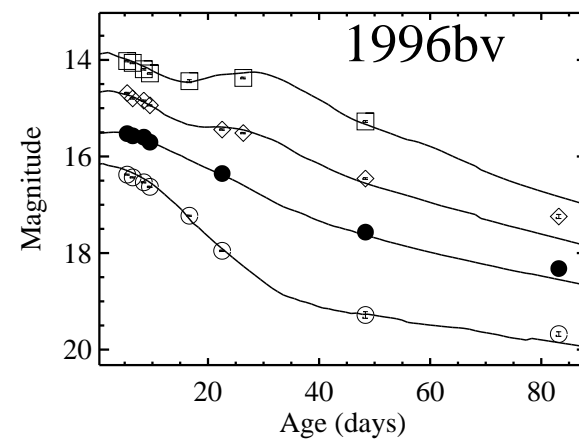
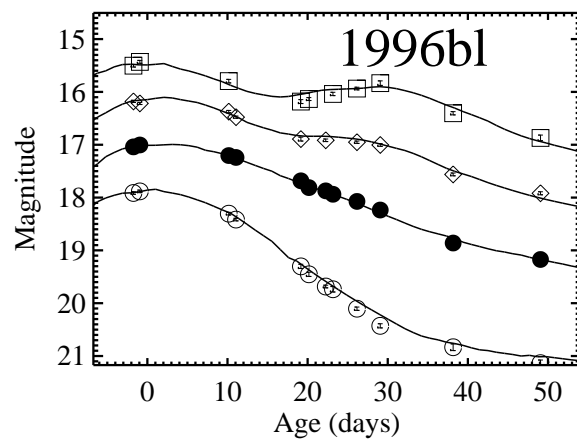
<http://arxiv.org/ps/astro-ph/9810291v1>

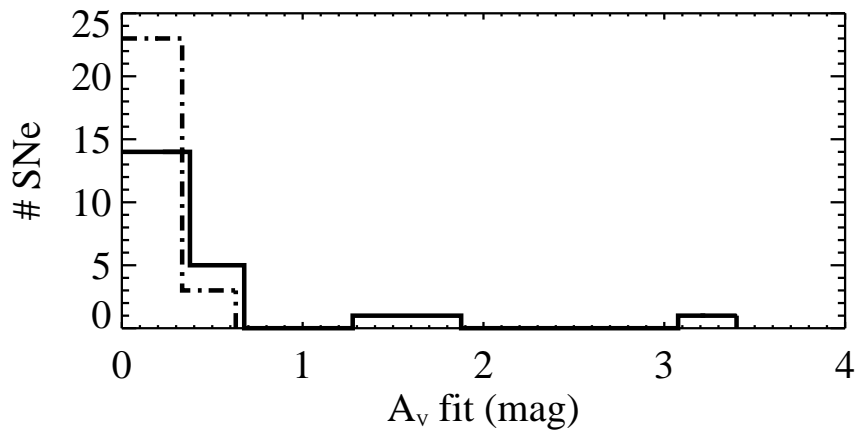
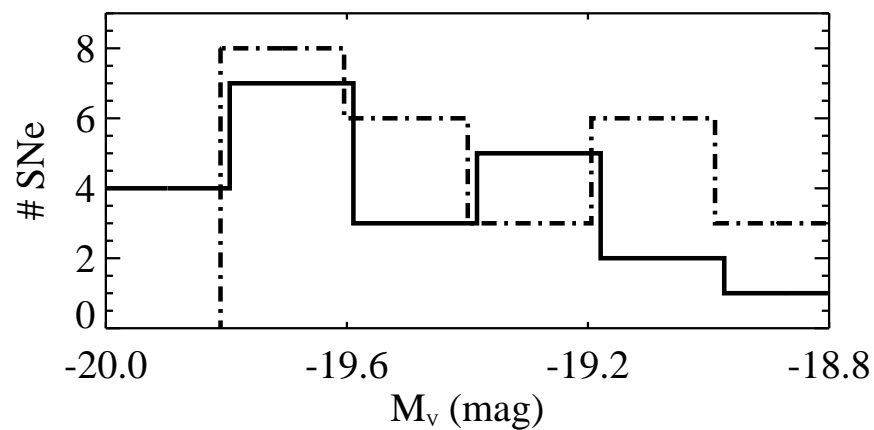
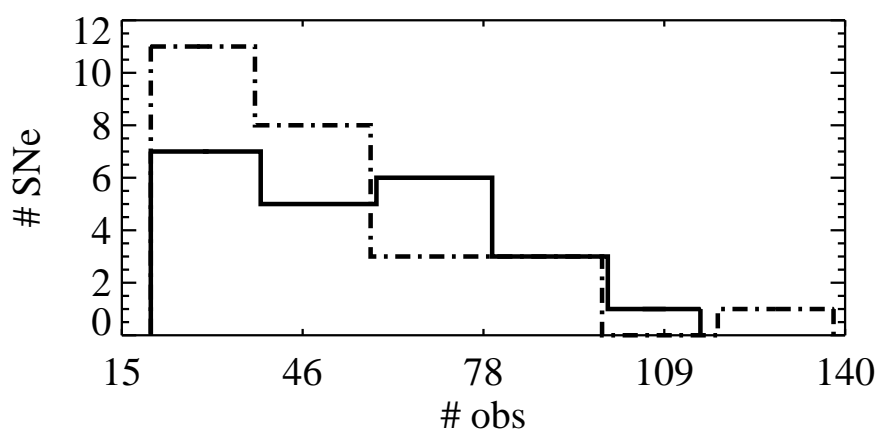
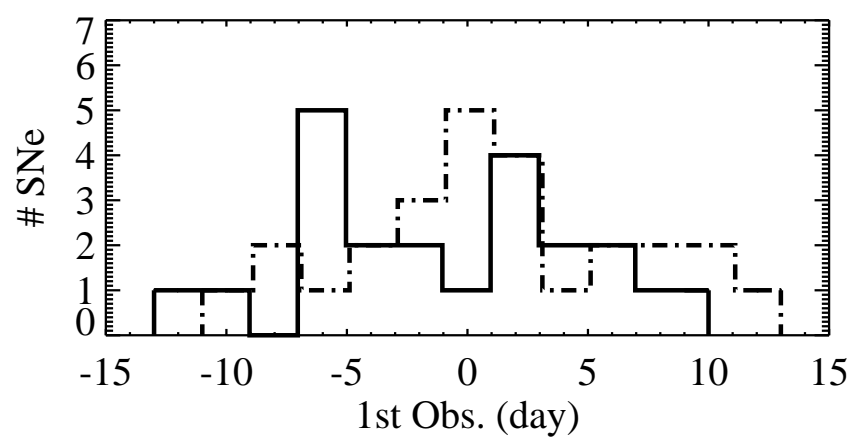
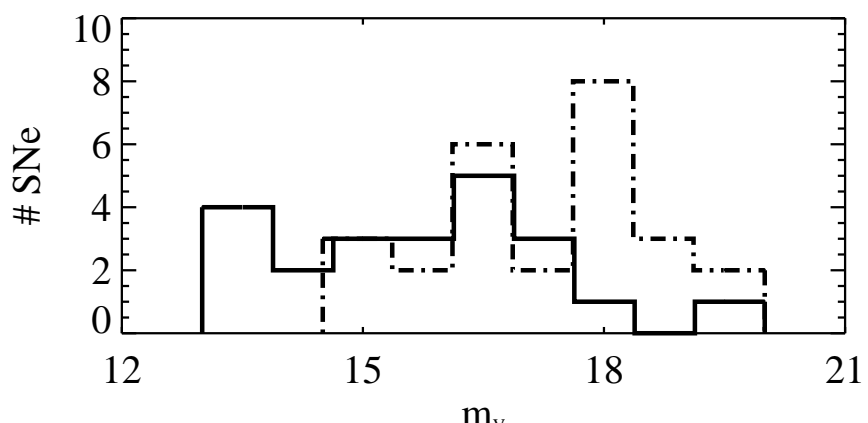
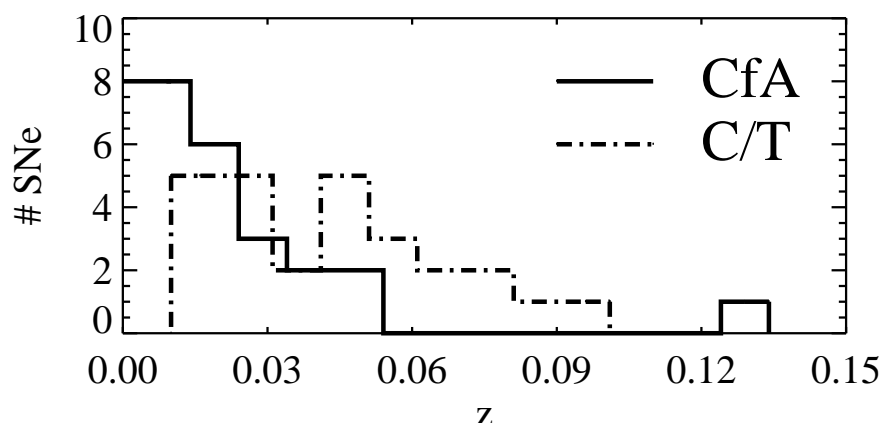
This figure "ariess.fig2.2.gif" is available in "gif" format from:

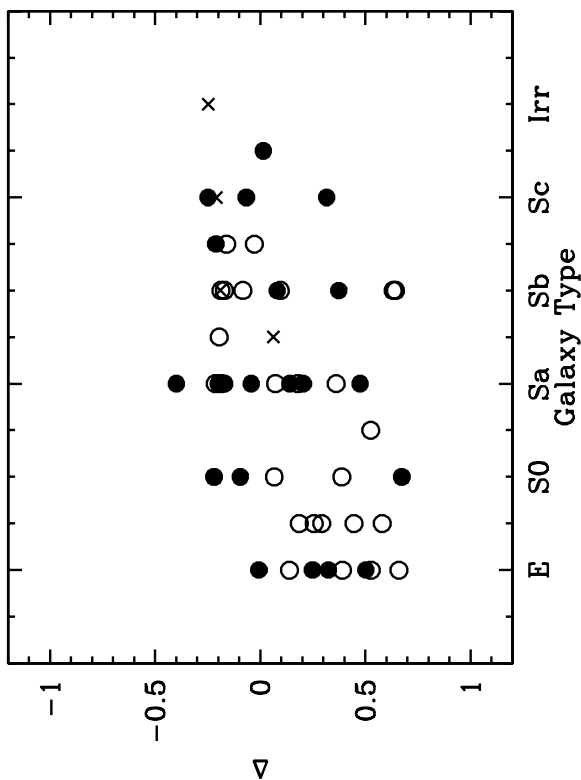
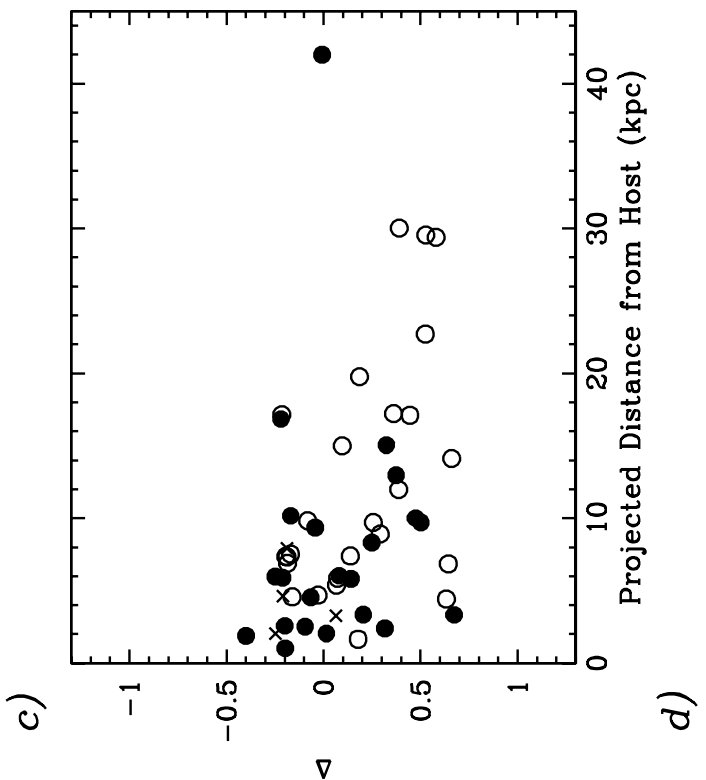
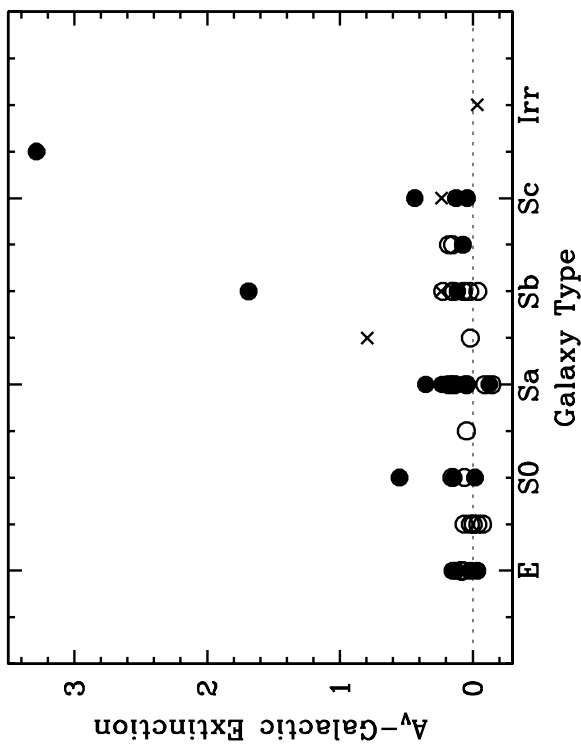
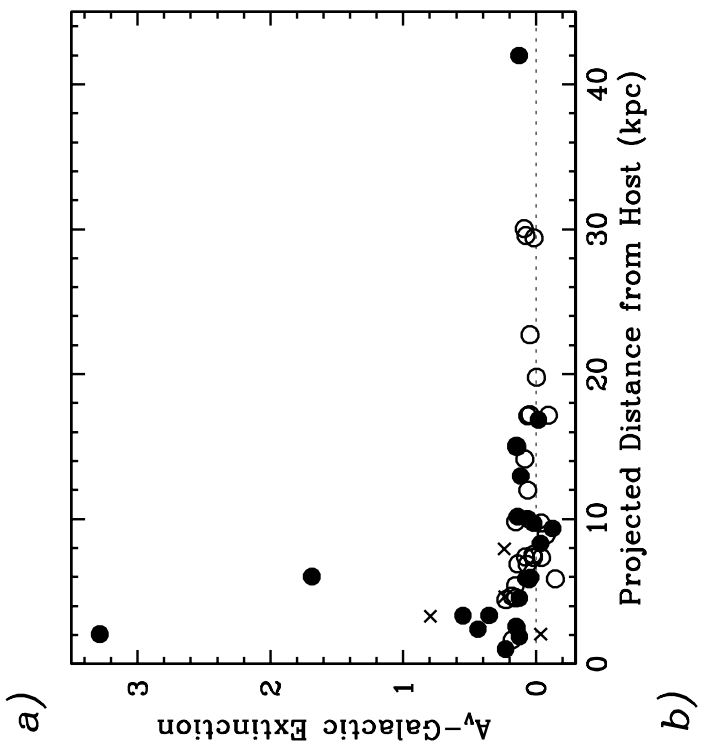
<http://arxiv.org/ps/astro-ph/9810291v1>

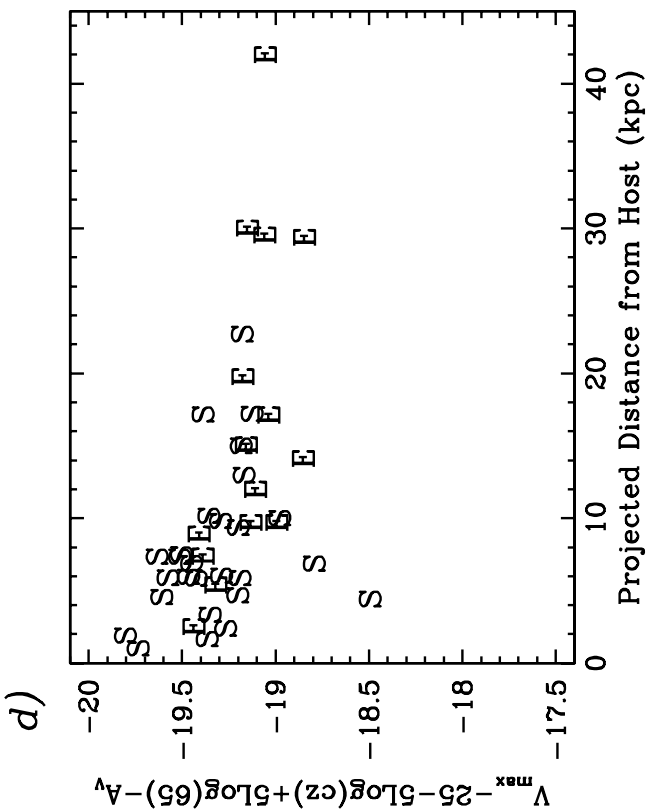
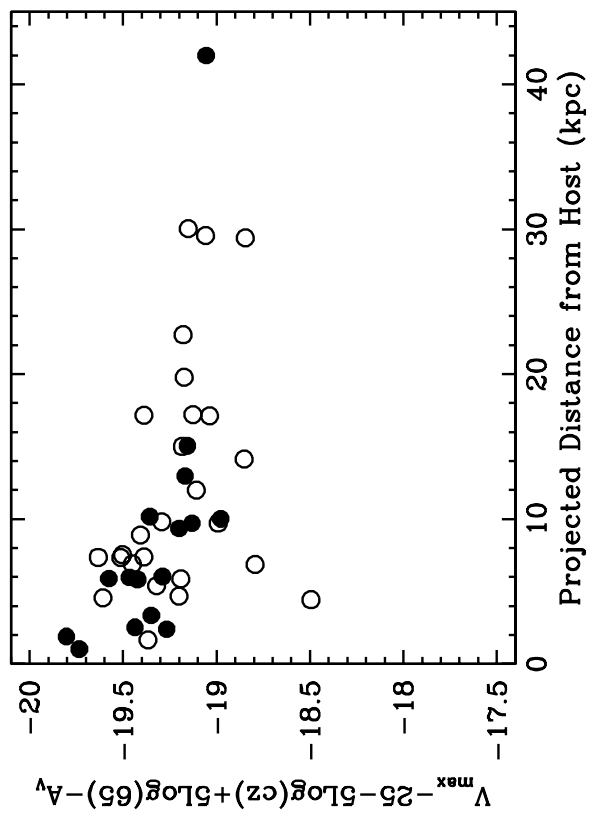
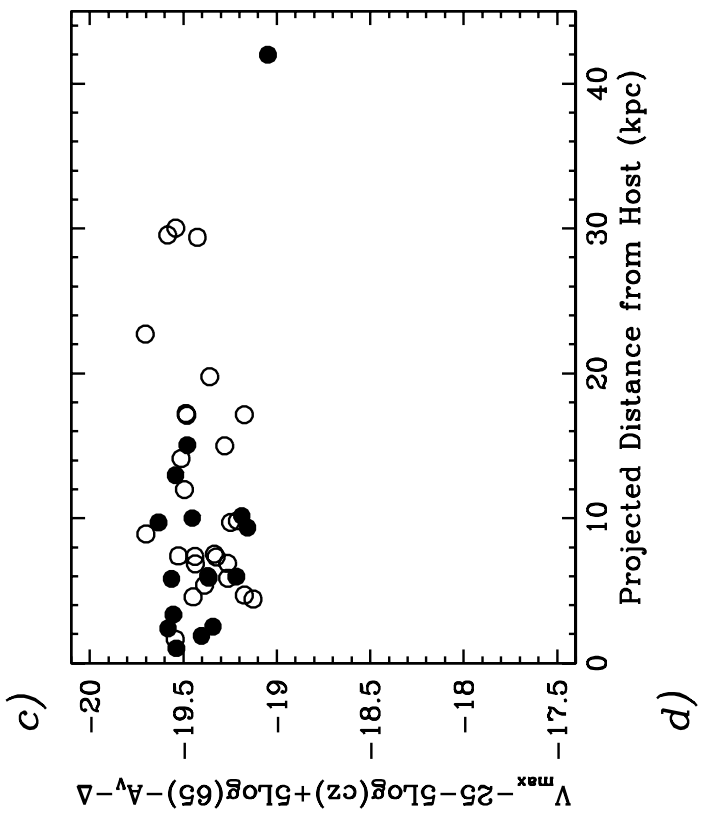
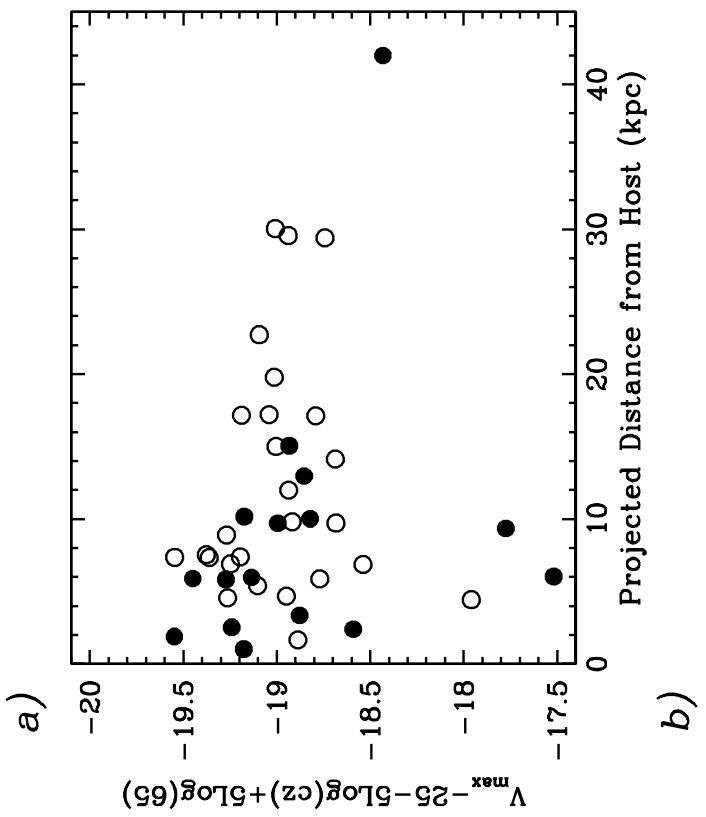


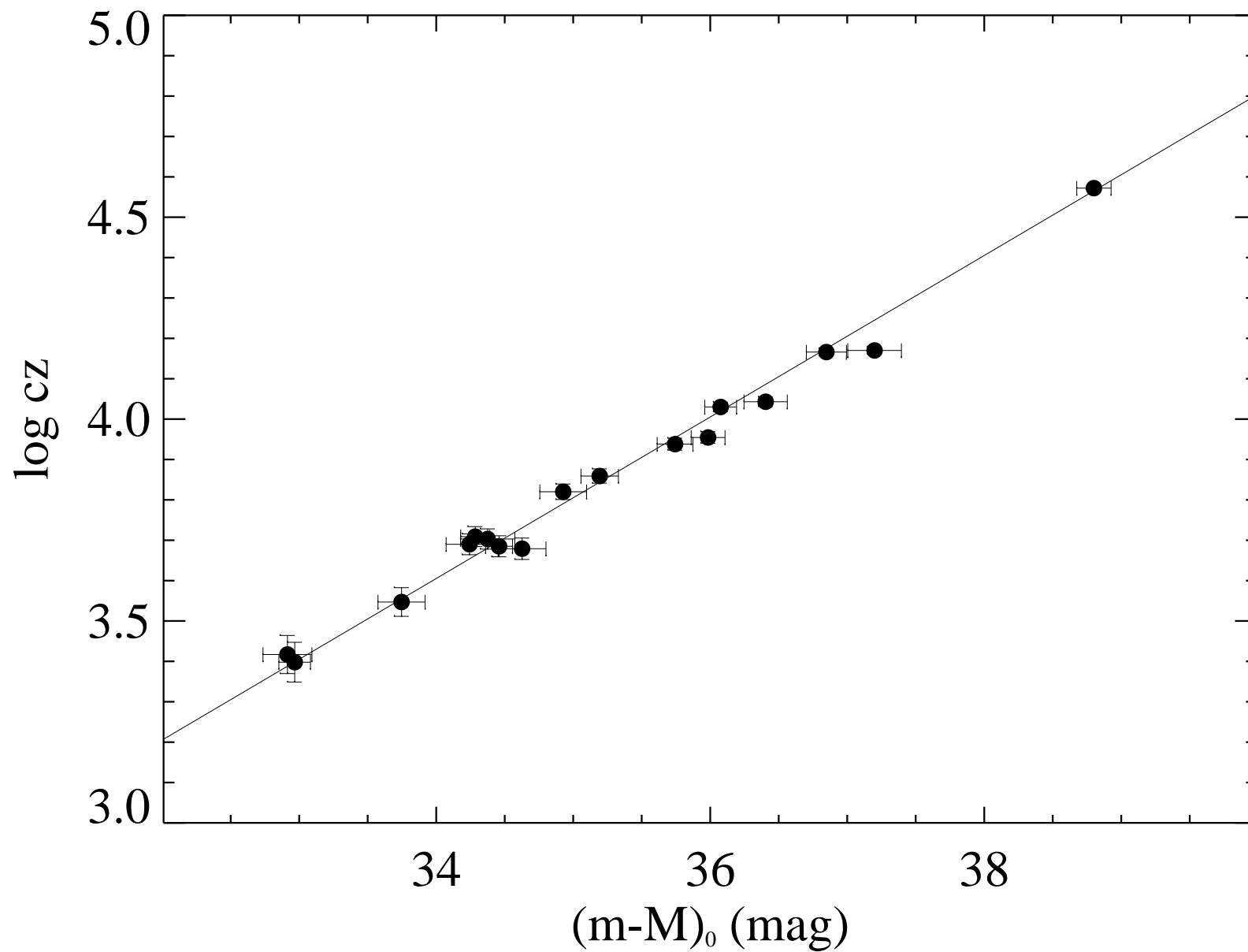












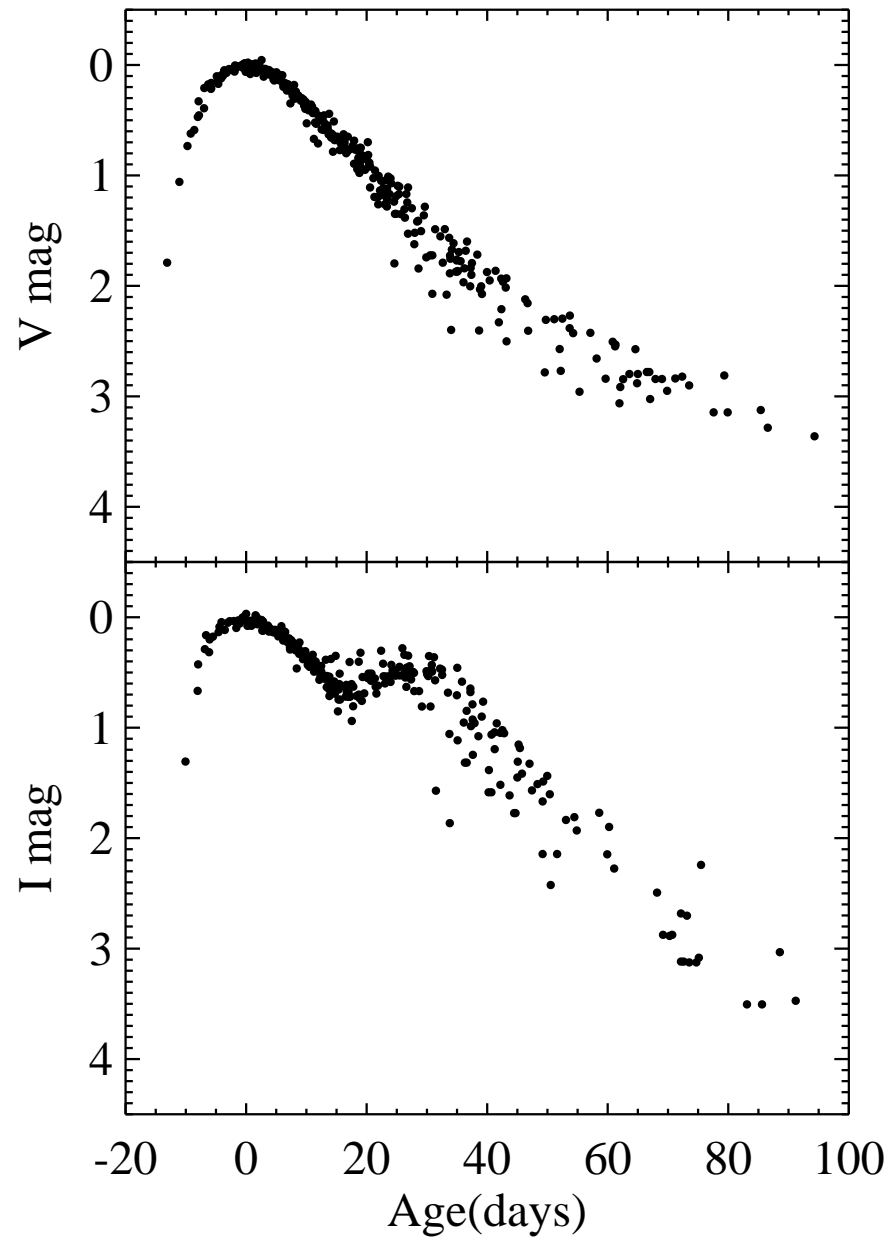
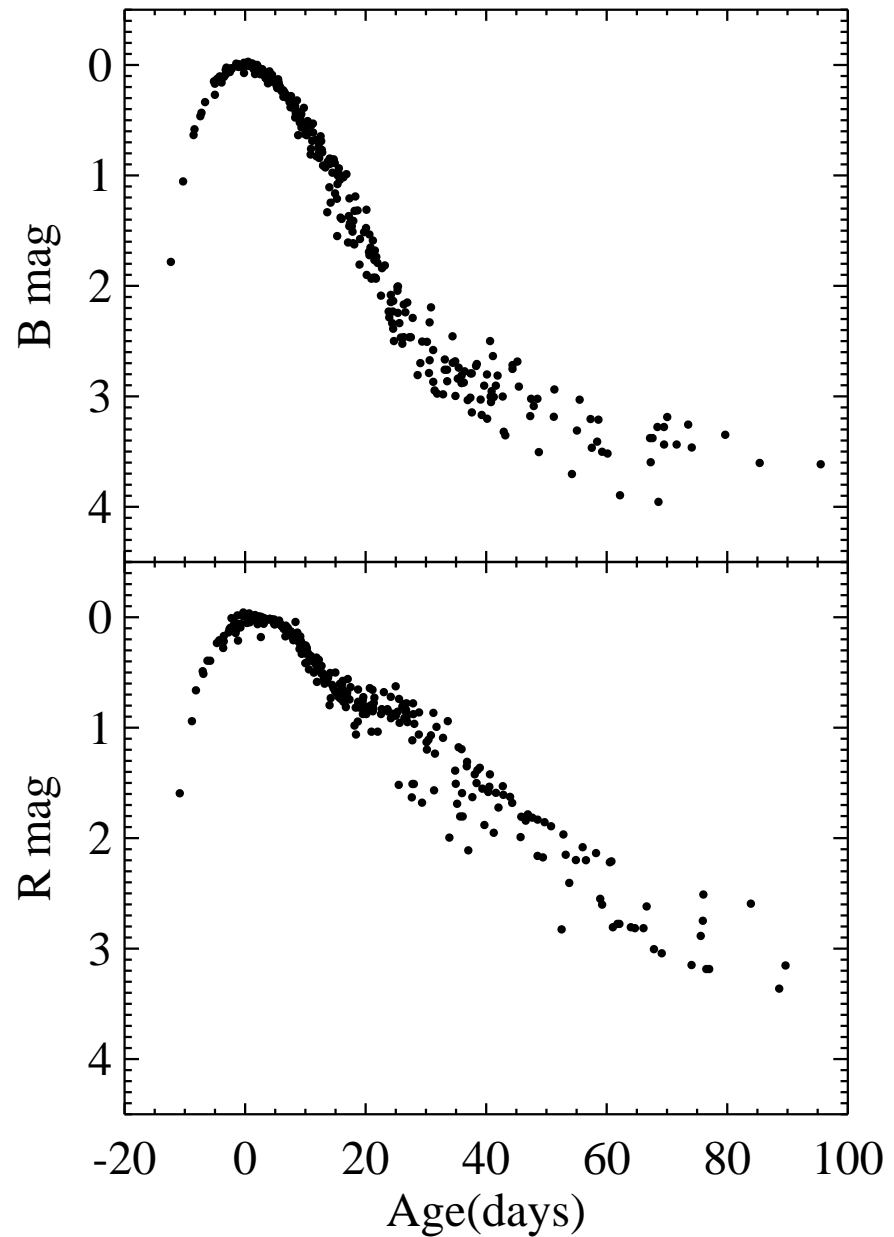


Table 6: Photometry of SN 1993ac

JD (2440000+)	B (mag)	V (mag)	R (mag)	I (mag)
9277.00	18.71 (0.02)	18.29 (0.07)	18.08 (0.02)	18.40 (0.03)
9284.10*	19.29 (0.09)	18.70 (0.04)	18.60 (0.05)	19.04 (0.20)
9285.80	19.68 (0.05)	18.92 (0.05)	18.62 (0.08)	18.89 (0.06)
9288.00	19.97 (0.05)	19.09 (0.04)	18.67 (0.05)	18.90 (0.10)
9295.90	—	19.47 (0.08)	18.88 (0.04)	18.65 (0.06)
9331.70	22.05 (0.07)	21.09 (0.07)	20.14 (0.04)	19.97 (0.07)

* photometry from CPO

Table 7: Photometry of SN 1993ae

JD (2440000+)	B (mag)	V (mag)	R (mag)	I (mag)
9302.60	16.59 (0.02)	16.04 (0.02)	—	16.32 (0.04)
9307.80	17.28 (0.02)	16.37 (0.02)	16.14 (0.02)	16.09 (0.02)
9311.70	17.75 (0.02)	16.66 (0.02)	16.29 (0.02)	16.06 (0.02)
9311.80*	17.76 (0.04)	16.68 (0.03)	16.34 (0.03)	16.11 (0.03)
9314.60	18.07 (0.05)	16.94 (0.02)	16.51 (0.02)	—
9315.70	18.18 (0.04)	17.01 (0.03)	16.57 (0.03)	16.25 (0.03)
9317.60	18.31 (0.05)	17.10 (0.05)	16.73 (0.05)	16.39 (0.04)
9323.60*	18.60 (0.06)	17.48 (0.04)	17.20 (0.04)	16.88 (0.04)
9327.70*	18.63 (0.05)	17.63 (0.03)	—	17.14 (0.04)
9331.70	18.74 (0.02)	17.77 (0.02)	17.49 (0.02)	17.32 (0.03)
9338.60*	18.86 (0.09)	—	—	17.68 (0.09)
9357.70*	19.22 (0.15)	18.53 (0.05)	18.46 (0.05)	18.39 (0.09)
9359.60	19.12 (0.09)	18.51 (0.04)	18.49 (0.04)	18.63 (0.09)
9361.70	19.28 (0.06)	18.57 (0.04)	18.55 (0.04)	18.67 (0.11)
9372.60*	—	18.85 (0.07)	18.92 (0.07)	19.05 (0.18)

* photometry from CPO

Table 8: Photometry of SN 1994M

JD (2440000+)	B (mag)	V (mag)	R (mag)	I (mag)
9476.76	—	16.29 (0.06)	—	—
9477.71	16.44 (0.03)	16.29 (0.03)	16.12 (0.03)	16.51 (0.03)
9479.72	16.51 (0.02)	16.35 (0.02)	16.13 (0.02)	16.57 (0.02)
9480.69	16.60 (0.03)	16.42 (0.03)	16.23 (0.03)	16.67 (0.03)
9481.78	—	16.38 (0.03)	16.19 (0.03)	16.63 (0.03)
9483.69	16.89 (0.03)	16.56 (0.03)	16.52 (0.03)	16.81 (0.03)
9484.77	16.97 (0.04)	16.61 (0.04)	16.55 (0.04)	16.92 (0.04)
9485.77	17.13 (0.04)	16.81 (0.04)	—	—
9489.66	17.60 (0.03)	16.92 (0.03)	16.87 (0.03)	17.03 (0.03)
9497.74	—	17.37 (0.12)	16.95 (0.12)	16.72 (0.12)
9500.69	18.95 (0.05)	17.59 (0.05)	17.19 (0.05)	16.81 (0.05)
9505.68	19.29 (0.05)	18.10 (0.05)	17.64 (0.05)	17.31 (0.05)
9508.75	19.40 (0.06)	18.15 (0.06)	17.76 (0.06)	17.49 (0.06)
9512.75	19.56 (0.07)	18.34 (0.07)	17.95 (0.07)	17.75 (0.07)
9514.71	19.62 (0.06)	18.40 (0.06)	18.02 (0.06)	17.84 (0.06)
9538.70	—	19.17 (0.07)	—	—
9542.67	20.02 (0.10)	19.16 (0.10)	19.14 (0.10)	19.11 (0.10)
9546.65	—	19.26 (0.15)	—	—

Table 9: Photometry of SN 1994S

JD (2440000+)	B (mag)	V (mag)	R (mag)	I (mag)
9513.70	14.99 (0.05)	15.04 (0.05)	14.99 (0.05)	15.19 (0.05)
9514.80	14.98 (0.03)	14.96 (0.03)	14.93 (0.03)	15.09 (0.03)
9515.70	14.86 (0.03)	14.93 (0.03)	14.96 (0.03)	15.20 (0.03)
9517.70	14.85 (0.06)	14.84 (0.06)	14.83 (0.06)	15.17 (0.06)
9519.70	14.85 (0.04)	14.85 (0.04)	14.82 (0.04)	15.28 (0.04)
9529.70*	15.40 (0.04)	15.21 (0.04)	—	15.87 (0.04)
9536.60**	—	15.65 (0.06)	15.88 (0.06)	15.88 (0.06)
9538.70	—	15.76 (0.05)	—	—
9541.70	16.73 (0.03)	15.89 (0.03)	15.74 (0.03)	15.82 (0.03)
9545.70	17.13 (0.03)	16.08 (0.03)	15.79 (0.03)	15.66 (0.03)
9547.70	—	16.19 (0.06)	—	—
9553.70	—	16.65 (0.10)	—	—

* photometry from McGraw Hill Observatory 1.3m

** photometry from McDonald Observatory

Table 10: Photometry of SN 1994T

JD (2440000+)	B (mag)	V (mag)	R (mag)	I (mag)
9514.80	17.47 (0.02)	17.24 (0.02)	17.26 (0.02)	17.44 (0.02)
9515.70	17.48 (0.04)	17.25 (0.04)	17.04 (0.04)	17.48 (0.04)
9516.80	17.59 (0.05)	17.25 (0.05)	17.09 (0.05)	17.51 (0.05)
9518.70	17.77 (0.05)	17.43 (0.05)	17.22 (0.05)	17.74 (0.05)
9524.60 [†]	18.59 (0.03)	17.78 (0.03)	17.08 (0.03)	18.15 (0.03)
9530.70*	18.88 (0.04)	18.15 (0.04)	17.85 (0.04)	17.72 (0.04)
9531.60**	—	18.21 (0.05)	—	—
9537.70	—	18.64 (0.08)	—	—
9538.70	—	18.82 (0.08)	—	—
9541.70	20.35 (0.08)	19.14 (0.05)	18.59 (0.05)	18.31 (0.05)
9545.70	—	19.38 (0.10)	18.75 (0.10)	—
9546.70	—	—	—	18.56(0.10)
9547.70	—	—	19.39(0.12)	—

[†] photometry from CTIO 1.0m

* photometry from McGraw Hill Observatory 1.3m

** photometry from McDonald Observatory

Table 11: Photometry of SN 1994Q

JD (2440000+)	B (mag)	V (mag)	R (mag)	I (mag)
9507.80	17.08 (0.04)	16.69 (0.04)	16.65 (0.04)	17.17 (0.04)
9508.80	17.13 (0.03)	16.75 (0.04)	16.72 (0.04)	17.21 (0.04)
9509.80	17.23 (0.03)	16.81 (0.04)	16.78 (0.04)	17.21 (0.04)
9511.80	17.46 (0.04)	16.94 (0.04)	16.91 (0.04)	17.25 (0.04)
9514.90	17.77 (0.04)	17.09 (0.04)	—	—
9516.70	—	17.16 (0.04)	17.00 (0.04)	17.18 (0.04)
9519.80	18.27 (0.05)	17.31 (0.04)	17.01 (0.04)	17.07 (0.04)
9521.80	—	17.46 (0.04)	17.02 (0.04)	17.13 (0.04)
9535.90	19.33 (0.07)	18.27 (0.08)	17.70 (0.08)	17.57 (0.08)
9542.80	19.52 (0.07)	18.51 (0.08)	17.98 (0.08)	18.02 (0.08)
9545.80	19.63 (0.07)	18.57 (0.08)	17.99 (0.08)	18.17 (0.08)
9564.70	—	19.18 (0.10)	—	—
9565.70	—	19.22 (0.10)	—	—

Table 12: Photometry of SN 1994ae

JD (2440000+)	B (mag)	V (mag)	R (mag)	I (mag)
9672.97	15.00 (0.02)	14.89 (0.03)	14.60 (0.02)	14.67 (0.04)
9674.96	14.27 (0.02)	14.16 (0.03)	13.94 (0.02)	14.03 (0.04)
9676.96	13.79 (0.02)	13.72 (0.03)	13.52 (0.02)	13.68 (0.03)
9678.00	13.64 (0.02)	13.57 (0.04)	13.40 (0.02)	—
9685.02	—	—	13.00 (0.03)	13.40 (0.04)
9686.00	13.19 (0.02)	13.09 (0.03)	13.00 (0.02)	13.40 (0.04)
9686.99	13.22 (0.02)	13.11 (0.03)	13.01 (0.02)	13.44 (0.04)
9688.04	13.30 (0.02)	—	—	13.48 (0.04)
9689.06	13.34(0.02)	—	—	—
9690.03	13.37 (0.02)	13.17 (0.03)	13.06 (0.02)	13.55 (0.05)
9694.03	13.61 (0.02)	13.35 (0.04)	13.26 (0.02)	13.79 (0.03)
9695.03	13.67 (0.02)	13.38 (0.03)	13.33 (0.02)	13.86 (0.05)
9695.98	13.76 (0.02)	13.43 (0.03)	13.42 (0.02)	13.92 (0.04)
9696.96	13.83 (0.02)	13.49 (0.03)	13.50 (0.02)	13.98 (0.04)
9699.98	14.12 (0.02)	13.70 (0.04)	13.70 (0.04)	14.09 (0.06)
9700.97	14.22 (0.02)	13.77 (0.04)	13.73 (0.04)	14.10 (0.04)
9702.96	14.44 (0.02)	13.84 (0.03)	13.78 (0.03)	14.07 (0.04)
9705.06	14.66 (0.02)	13.96 (0.03)	13.80 (0.03)	14.01 (0.06)
9707.06	14.82 (0.04)	14.04 (0.06)	13.84 (0.03)	13.99 (0.06)
9715.93	15.74 (0.04)	14.51 (0.05)	14.07 (0.04)	13.87 (0.07)
9721.02	16.07 (0.04)	14.80 (0.05)	14.35 (0.05)	14.08 (0.07)
9725.01	—	15.03 (0.05)	14.58 (0.05)	14.36 (0.05)
9726.98	16.28 (0.04)	15.08 (0.05)	—	14.52 (0.07)
9736.86	—	15.43 (0.07)	—	—
9740.85	16.54 (0.04)	15.55 (0.05)	15.20 (0.05)	15.16 (0.07)
9744.94	16.62 (0.04)	15.64 (0.05)	15.34 (0.05)	15.31 (0.05)
9745.91	16.63 (0.04)	15.67 (0.05)	15.37 (0.06)	15.36 (0.05)
9749.99	16.66 (0.04)	15.77 (0.05)	—	—
9769.74	16.93 (0.05)	16.27 (0.06)	16.09 (0.06)	16.31 (0.07)
9783.86	17.14 (0.05)	16.62 (0.07)	16.51 (0.00)	—
9805.88	17.51 (0.08)	17.06 (0.08)	17.14 (0.08)	17.46 (0.08)
9843.80	18.05(0.05)	17.83(0.05)	18.11(0.05)	—

Table 13: Photometry of SN 1995D

JD (2440000+)	B (mag)	V (mag)	R (mag)	I (mag)
9762.08	—	13.74 (0.05)	—	—
9765.74*	13.53 (0.05)	13.51 (0.05)	13.52 (0.05)	13.70 (0.05)
9765.87	13.52 (0.04)	13.53 (0.06)	13.46 (0.05)	13.70 (0.06)
9766.79	13.47 (0.04)	13.49 (0.03)	13.43 (0.03)	13.68 (0.04)
9767.67*	13.47 (0.05)	13.47 (0.05)	13.47 (0.05)	13.70 (0.05)
9769.79	13.42 (0.05)	13.40 (0.03)	13.38 (0.05)	13.71 (0.04)
9770.68*	13.50 (0.06)	13.43 (0.05)	13.48 (0.06)	13.81 (0.05)
9771.82	13.47 (0.05)	13.43 (0.05)	13.39 (0.05)	13.82 (0.04)
9772.69	13.56 (0.05)	13.46 (0.04)	13.44 (0.04)	13.86 (0.04)
9773.78	13.58 (0.04)	13.49 (0.04)	13.44 (0.04)	13.88 (0.05)
9775.95	13.72 (0.06)	13.54 (0.07)	13.54 (0.05)	13.98 (0.05)
9776.66	13.78 (0.06)	13.58 (0.06)	13.59 (0.05)	14.01 (0.05)
9776.67*	13.77 (0.04)	13.58 (0.04)	13.65 (0.05)	14.07 (0.05)
9779.74	13.99 (0.04)	13.72 (0.03)	13.77 (0.03)	14.20 (0.04)
9780.88	14.13 (0.06)	13.79 (0.04)	13.88 (0.03)	14.26 (0.04)
9781.66	14.20 (0.03)	13.84 (0.04)	13.92 (0.03)	14.29 (0.05)
9783.77	14.43 (0.03)	13.97 (0.03)	14.03 (0.03)	14.33 (0.05)
9784.72*	14.53 (0.05)	14.03 (0.05)	14.10 (0.05)	14.41 (0.05)
9784.77	14.54 (0.03)	14.06 (0.03)	14.08 (0.03)	—
9785.70*	14.64 (0.04)	14.09 (0.04)	14.12 (0.05)	14.39 (0.06)
9787.69	14.86 (0.04)	14.19 (0.02)	14.13 (0.03)	14.26 (0.04)
9792.67*	15.35 (0.04)	14.50 (0.04)	14.23 (0.04)	14.24 (0.04)
9795.73	15.63 (0.04)	14.55 (0.04)	14.26 (0.03)	14.20 (0.05)
9799.63	15.97 (0.04)	14.75 (0.03)	14.37 (0.04)	14.16 (0.04)
9803.63	16.13 (0.04)	14.93 (0.03)	14.55 (0.03)	14.28 (0.04)
9805.74	16.27 (0.04)	15.06 (0.03)	14.69 (0.04)	14.34 (0.06)
9806.78	16.33 (0.07)	15.13 (0.07)	—	14.45 (0.04)
9810.73	16.47 (0.04)	15.32 (0.03)	14.98 (0.03)	14.74 (0.04)
9812.65	16.47 (0.04)	15.38 (0.04)	15.06 (0.03)	14.84 (0.04)
9820.69	16.64 (0.04)	15.63 (0.04)	15.34 (0.07)	15.18 (0.07)
9827.72	16.75 (0.04)	15.82 (0.04)	15.58 (0.03)	15.54 (0.05)
9829.67	16.76 (0.04)	15.86 (0.04)	15.63 (0.04)	15.62 (0.05)
9835.68	16.83 (0.04)	16.00 (0.04)	15.82 (0.04)	15.86 (0.08)
9843.70	16.96 (0.04)	16.23 (0.05)	16.23 (0.04)	16.18 (0.08)
9851.63	17.04 (0.05)	16.39 (0.05)	16.27 (0.05)	16.37 (0.08)

* photometry from CPO

Table 14: Photometry of SN 1995E

JD (2440000+)	B (mag)	V (mag)	R (mag)	I (mag)
9772.70	16.85 (0.05)	16.16 (0.04)	15.60 (0.03)	15.32 (0.04)
9773.80	16.83 (0.04)	16.11 (0.05)	15.60 (0.03)	15.37 (0.04)
9776.70	16.85 (0.05)	16.09 (0.03)	15.59 (0.04)	15.46 (0.04)
9779.60	16.97 (0.04)	16.12 (0.05)	15.55 (0.04)	15.56 (0.05)
9780.90	17.04 (0.08)	16.14 (0.05)	15.61 (0.03)	15.59 (0.04)
9781.60	17.07 (0.04)	16.22 (0.03)	15.70 (0.04)	15.63 (0.04)
9783.70	17.27 (0.04)	16.25 (0.04)	15.81 (0.02)	15.76 (0.04)
9784.70	17.39 (0.04)	16.34 (0.06)	15.94 (0.04)	—
9787.70	17.61 (0.05)	16.46 (0.05)	16.10 (0.04)	15.99 (0.05)
9791.70	18.24 (0.09)	16.73 (0.05)	16.28 (0.03)	16.07 (0.07)
9799.60	19.01 (0.07)	17.16 (0.05)	16.42 (0.03)	15.82 (0.05)
9803.60	—	17.36 (0.06)	16.60 (0.04)	15.88 (0.05)
9805.70	19.19 (0.10)	17.53 (0.08)	—	—
9806.60	19.44 (0.11)	17.62 (0.06)	16.77 (0.05)	16.04 (0.04)
9810.80	19.54 (0.20)	17.84 (0.07)	—	16.34 (0.05)
9811.60	19.63 (0.10)	—	—	—
9812.60	19.87 (0.10)	17.90 (0.06)	17.16 (0.05)	16.43 (0.05)
9820.70	19.86 (0.13)	18.18 (0.06)	17.53 (0.06)	16.91 (0.06)
9828.70	—	18.41 (0.08)	17.69 (0.05)	17.27 (0.10)
9843.60	—	18.67 (0.08)	18.19 (0.07)	—
9850.70	—	18.98 (0.10)	18.45 (0.09)	18.43 (0.09)
9864.70	—	19.36 (0.15)	18.93 (0.10)	18.82 (0.06)

Table 15: Photometry of SN 1995al

JD (2440000+)	B (mag)	V (mag)	R (mag)	I (mag)
10025.00	13.45(0.04)	13.41(0.04)	13.36(0.04)	13.53(0.04)
10030.00	13.36(0.04)	13.25(0.04)	13.21(0.04)	13.55(0.04)
10031.00	13.44(0.06)	13.26(0.06)	13.28(0.06)	13.61(0.06)
10032.00	13.42(0.04)	13.26(0.04)	13.23(0.04)	13.62(0.04)
10034.90	13.57(0.03)	13.28(0.05)	13.33(0.05)	13.62(0.05)
10035.00	13.56(0.06)	13.30(0.06)	13.35(0.06)	13.72(0.06)
10037.00	13.64(0.06)	13.33(0.06)	13.45(0.04)	13.83(0.04)
10037.00	13.64(0.06)	13.36(0.05)	13.45(0.04)	13.83(0.04)
10038.00	13.73(0.04)	13.41(0.04)	13.52(0.04)	13.88(0.04)
10039.90	13.87(0.03)	13.50(0.05)	13.58(0.05)	13.90(0.05)
10042.00	14.05(0.03)	13.65(0.05)	13.72(0.05)	14.04(0.05)
10045.00	14.34(0.04)	13.80(0.04)	13.90(0.04)	14.12(0.04)
10048.00	14.69(0.04)	13.95(0.04)	13.95(0.04)	14.04(0.04)
10051.00	15.05(0.04)	14.00(0.06)	13.90(0.07)	13.92(0.07)
10054.80	15.42(0.03)	14.30(0.05)	14.00(0.05)	13.84(0.05)
10067.00	16.24(0.03)	14.95(0.03)	14.61(0.03)	14.28(0.03)
10070.90	16.33(0.03)	15.13(0.03)	14.81(0.03)	14.51(0.03)
10078.90	16.46(0.03)	15.41(0.03)	15.11(0.03)	14.92(0.03)
10087.00	16.58(0.03)	15.64(0.03)	15.36(0.03)	15.25(0.03)
10088.90	16.59(0.03)	15.68(0.03)	15.43(0.03)	15.36(0.03)
100103.80	16.84(0.03)	16.08(0.03)	15.91(0.04)	15.80(0.04)
100136.90	17.28(0.04)	16.88(0.04)	16.91(0.06)	17.14(0.06)
100161.70	17.80(0.07)	17.44(0.07)	17.68(0.10)	17.98(0.11)

Table 16: Photometry of SN 1995ac

JD (2440000+)	B (mag)	V (mag)	R (mag)	I (mag)
9987.64	17.30(0.03)	17.36(0.03)	17.34(0.04)	17.37(0.03)
9988.77	17.27(0.04)	17.30(0.03)	17.32(0.03)	17.35(0.03)
9989.75	17.19(0.03)	17.26(0.04)	17.21(0.04)	17.32(0.02)
9992.71	17.28(0.03)	17.23(0.03)	17.14(0.04)	17.32(0.03)
9994.63	17.28(0.04)	17.24(0.03)	—	17.32(0.04)
9998.65	17.40(0.04)	17.24(0.03)	17.15(0.04)	17.41(0.05)
10000.60	17.59(0.02)	17.33(0.03)	17.22(0.03)	17.52(0.02)
10001.60	17.60(0.03)	17.36(0.02)	17.27(0.04)	17.51(0.03)
10002.70	17.64(0.04)	17.38(0.03)	17.34(0.04)	17.58(0.02)
10004.70	17.80(0.03)	17.51(0.03)	17.45(0.03)	17.66(0.03)
10005.70	17.93(0.03)	17.56(0.03)	17.50(0.03)	17.67(0.02)
10007.70	18.14(0.03)	17.67(0.03)	17.55(0.04)	17.71(0.05)
10008.70	18.26(0.03)	17.70(0.03)	17.64(0.03)	17.71(0.04)
10009.70	18.37(0.03)	17.78(0.03)	17.63(0.03)	17.68(0.05)
10011.70	18.63(0.03)	17.93(0.03)	17.74(0.03)	17.74(0.03)
10013.70	18.87(0.03)	18.04(0.02)	17.75(0.03)	17.67(0.03)
10017.60	19.16(0.03)	18.24(0.03)	17.74(0.06)	17.66(0.04)
10026.60	20.02(0.03)	18.83(0.03)	18.06(0.03)	—
10029.60	20.09(0.04)	18.91(0.03)	18.32(0.03)	18.01(0.03)
10031.60	20.06(0.03)	18.96(0.02)	18.49(0.03)	18.14(0.03)
10033.70	20.16(0.03)	19.08(0.04)	18.54(0.05)	18.18(0.07)
10048.70	20.39(0.04)	19.57(0.05)	19.19(0.05)	18.95(0.05)

Table 17: Photometry of SN 1995ak

JD (2440000+)	B (mag)	V (mag)	R (mag)	I (mag)
10024.79	16.17(0.05)	16.13(0.05)	15.82(0.06)	16.26(0.08)
10025.82	16.19(0.06)	16.12(0.05)	15.86(0.04)	16.29(0.10)
10026.70	16.18(0.08)	16.01(0.09)	15.94(0.08)	16.33(0.13)
10031.71	16.77(0.05)	16.41(0.05)	16.41(0.05)	16.74(0.09)
10035.67	—	16.73(0.04)	16.67(0.06)	16.85(0.07)
10036.62	17.48(0.06)	16.78(0.05)	16.63(0.07)	16.76(0.09)
10038.63	17.72(0.08)	16.88(0.06)	16.42(0.04)	—
10039.82	17.76(0.04)	16.86(0.04)	16.57(0.04)	—
10047.58	18.68(0.12)	17.40(0.08)	16.82(0.11)	16.54(0.14)
10048.57	18.65(0.05)	17.33(0.07)	16.84(0.06)	16.48(0.07)
10052.62	18.99(0.02)	17.75(0.04)	17.09(0.08)	16.49(0.05)
10066.72	19.54(0.06)	18.34(0.03)	17.87(0.03)	17.32(0.05)
10071.64	19.68(0.05)	18.52(0.03)	18.10(0.03)	17.82(0.06)
10077.69	19.88(0.05)	18.68(0.04)	18.25(0.03)	18.12(0.03)
10086.67	20.08(0.05)	19.01(0.04)	18.74(0.04)	18.46(0.08)
10091.72	20.14(0.05)	19.11(0.03)	18.91(0.03)	18.68(0.03)

Table 18: Photometry of SN 1995bd

JD (2440000+)	B (mag)	V (mag)	R (mag)	I (mag)
10077.80	17.91(0.02)	17.22(0.03)	16.73(0.03)	16.43(0.03)
10078.89	17.74(0.02)	17.07(0.02)	16.56(0.03)	16.30(0.03)
10079.75	17.61(0.02)	16.94(0.02)	16.46(0.03)	16.23(0.02)
10081.66	17.40(0.02)	16.70(0.02)	16.27(0.04)	16.07(0.02)
10087.72	17.29(0.03)	16.49(0.02)	16.06(0.03)	16.07(0.02)
10088.71	17.36(0.03)	16.51(0.02)	16.08(0.03)	16.16(0.04)
10089.74	17.37(0.02)	16.50(0.03)	16.08(0.03)	16.14(0.02)
10091.82	17.50(0.02)	16.58(0.02)	16.08(0.03)	16.14(0.03)
10095.70	17.77(0.02)	16.76(0.03)	16.32(0.03)	16.40(0.03)
10096.62	17.83(0.03)	16.80(0.02)	16.38(0.03)	16.47(0.02)
10099.58	18.11(0.03)	17.03(0.02)	16.66(0.03)	16.62(0.05)
10100.62	18.16(0.03)	17.09(0.02)	16.67(0.03)	16.66(0.03)
10101.61	18.21(0.02)	17.14(0.03)	16.75(0.03)	16.69(0.03)
10102.82	18.34(0.04)	17.20(0.03)	16.81(0.04)	16.72(0.03)
10106.79	18.64(0.02)	17.36(0.03)	16.90(0.04)	16.66(0.03)
10117.61	19.54(0.04)	17.83(0.03)	16.93(0.03)	16.43(0.05)
10129.59	20.07(0.02)	18.39(0.02)	17.59(0.04)	17.09(0.02)
10131.63	20.06(0.03)	18.48(0.03)	17.69(0.02)	17.23(0.05)
10162.64	20.61(0.04)	19.33(0.03)	18.62(0.03)	18.29(0.03)
10182.64	20.91(0.07)	19.86(0.04)	—	—

Table 19: Photometry of SN 1996C

JD (2440000+)	B (mag)	V (mag)	R (mag)	I (mag)
10130.94	—	16.52(0.05)	—	—
10131.90	16.75(0.03)	16.53(0.05)	16.39(0.06)	16.88(0.03)
10132.86	16.81(0.03)	16.63(0.04)	16.44(0.06)	16.92(0.03)
10133.95	16.87(0.03)	16.60(0.04)	16.46(0.06)	16.94(0.03)
10135.88	—	16.66(0.04)	16.54(0.05)	17.06(0.02)
10136.98	17.01(0.02)	16.75(0.05)	16.65(0.06)	—
10141.97	17.34(0.03)	17.00(0.05)	17.00(0.06)	17.45(0.03)
10142.95	17.48(0.03)	17.08(0.04)	17.10(0.06)	17.51(0.03)
10148.90	—	17.40(0.05)	—	—
10150.93	18.32(0.02)	17.47(0.04)	17.24(0.06)	17.36(0.03)
10151.75	18.50(0.03)	17.57(0.04)	17.21(0.04)	17.41(0.04)
10154.01	18.66(0.02)	17.64(0.05)	17.27(0.06)	17.32(0.03)
10159.86	19.13(0.02)	17.99(0.05)	17.45(0.06)	17.29(0.03)
10165.91	19.53(0.03)	18.40(0.05)	17.91(0.06)	17.70(0.03)
10172.85	19.65(0.02)	18.58(0.05)	18.16(0.06)	18.06(0.03)
10182.83	19.77(0.02)	18.90(0.05)	18.55(0.05)	18.54(0.02)
10202.84	20.04(0.02)	19.44(0.05)	19.18(0.06)	19.46(0.03)
10216.75	20.36(0.02)	19.66(0.05)	19.59(0.06)	19.79(0.02)

Table 20: Photometry of SN 1996X

JD (2440000+)	B (mag)	V (mag)	R (mag)	I (mag)
10187.80	13.38(0.03)	13.39(0.03)	13.27(0.03)	13.36(0.02)
10188.80	13.34(0.02)	13.27(0.02)	13.28(0.02)	13.40(0.02)
10191.80	13.26(0.04)	13.22(0.03)	13.18(0.02)	13.45(0.02)
10192.80	13.29(0.03)	13.22(0.02)	13.17(0.03)	13.49(0.03)
10194.80	13.36(0.03)	13.25(0.03)	13.18(0.02)	13.52(0.02)
10195.80	13.42(0.03)	13.26(0.02)	13.20(0.03)	13.60(0.02)
10197.80	13.57(0.03)	13.33(0.03)	13.33(0.03)	13.71(0.04)
10199.80	13.76(0.03)	13.42(0.02)	13.50(0.02)	13.84(0.03)
10200.80	13.85(0.03)	13.46(0.02)	13.57(0.03)	13.92(0.04)
10202.80	14.10(0.03)	13.62(0.02)	13.75(0.02)	—
10210.80	15.10(0.03)	14.13(0.02)	13.98(0.02)	13.95(0.03)
10211.70	15.20(0.02)	14.18(0.03)	14.00(0.02)	13.93(0.03)
10215.70	15.59(0.03)	14.42(0.03)	14.07(0.03)	13.89(0.03)
10216.70	15.69(0.03)	14.48(0.02)	14.13(0.03)	13.89(0.03)
10220.70	16.00(0.02)	14.77(0.03)	14.37(0.03)	13.95(0.05)
10226.60	16.30(0.04)	15.14(0.02)	14.77(0.05)	14.34(0.05)
10239.65	16.62(0.03)	15.57(0.02)	15.33(0.03)	14.97(0.05)
10251.65	16.81(0.02)	15.90(0.02)	15.77(0.03)	15.64(0.05)

Table 21: Photometry of SN 1996Z

JD (2440000+)	B (mag)	V (mag)	R (mag)	I (mag)
10221.60	—	14.26(0.03)	14.13(0.03)	—
10222.60	14.80(0.03)	14.29(0.02)	14.17(0.03)	—
10223.60	14.87(0.03)	14.32(0.02)	14.24(0.03)	—
10224.60	14.93(0.03)	14.36(0.02)	14.28(0.04)	—
10225.60	15.03(0.03)	14.41(0.02)	14.39(0.02)	—
10230.60	15.56(0.03)	14.74(0.03)	14.74(0.03)	—
10280.40	18.18(0.10)	16.77(0.11)	—	—

Table 22: Photometry of SN 1996ab

JD (2440000+)	B (mag)	V (mag)	R (mag)	I (mag)
10225.80	19.74(0.03)	19.51(0.04)	—	—
10226.80	19.77(0.03)	19.51(0.03)	—	—
10228.96	19.84(0.04)	19.61(0.03)	—	—
10229.70	—	19.66(0.03)	—	—
10230.80	20.07(0.03)	19.66(0.03)	—	—
10239.80	20.83(0.07)	20.27(0.04)	—	—
10240.80	20.91(0.08)	20.33(0.04)	—	—
10241.80	—	20.44(0.05)	—	—
10242.80 [†]	21.14(0.13)	20.52(0.05)	—	—
10243.80	21.16(0.12)	20.51(0.05)	—	—
10245.70	21.67(0.22)	20.67(0.07)	—	—
10247.90 [†]	21.80(0.25)	21.00(0.09)	—	—
10248.80 [†]	21.87(0.25)	21.10(0.10)	—	—
10249.80	22.24(0.32)	20.98(0.12)	—	—
10251.80	22.29(0.32)	21.11(0.21)	—	—
10280.80	—	22.85(0.20)	—	—
10283.70 [†]	—	22.64(0.20)	—	—

[†] photometry from MDM 2.3m

Table 23: Photometry of SN 1996bl

JD (2440000+)	B (mag)	V (mag)	R (mag)	I (mag)
10373.8	17.11(0.02)	17.04(0.02)	16.88(0.02)	17.10(0.03)
10374.6	17.08(0.02)	17.00(0.02)	16.92(0.02)	17.03(0.03)
10385.7	17.50(0.03)	17.20(0.02)	17.07(0.02)	17.40(0.03)
10386.6	17.62(0.02)	17.24(0.02)	17.18(0.02)	—
10394.7	18.50(0.04)	17.68(0.02)	17.59(0.04)	17.78(0.04)
10395.7	18.65(0.04)	17.81(0.03)	—	17.74(0.03)
10397.8	18.88(0.03)	17.87(0.03)	17.62(0.03)	—
10398.7	18.94(0.05)	17.94(0.02)	—	17.64(0.03)
10401.7	19.30(0.03)	18.07(0.02)	17.65(0.02)	17.54(0.03)
10404.6	19.63(0.04)	18.24(0.03)	17.70(0.03)	17.43(0.04)
10413.7	20.03(0.06)	18.86(0.03)	18.26(0.03)	18.00(0.03)
10424.6	20.33(0.06)	19.17(0.03)	18.62(0.03)	18.47(0.05)

Table 24: Photometry of SN 1996bo

JD (2440000+)	B (mag)	V (mag)	R (mag)	I (mag)
10381.7	16.42(0.02)	16.15(0.01)	15.74(0.01)	15.73(0.01)
10385.7	16.16(0.02)	15.81(0.01)	15.46(0.01)	15.67(0.01)
10386.6	16.15(0.02)	15.79(0.01)	15.46(0.01)	15.72(0.01)
10388.6	16.22(0.02)	15.75(0.01)	15.46(0.01)	15.71(0.01)
10392.6	16.37(0.02)	15.84(0.01)	15.57(0.01)	15.81(0.01)
10394.7	16.57(0.02)	15.91(0.01)	15.67(0.01)	15.96(0.01)
10396.8	16.81(0.02)	16.06(0.01)	15.84(0.01)	16.09(0.01)
10398.8	17.02(0.02)	16.14(0.01)	16.01(0.01)	16.15(0.01)
10401.8	17.37(0.02)	16.37(0.01)	16.13(0.01)	16.22(0.01)
10405.8	17.84(0.02)	16.55(0.01)	16.22(0.01)	16.11(0.01)
10412.7	18.47(0.04)	16.94(0.02)	16.31(0.01)	15.99(0.01)
10427.7	18.72(0.03)	18.23(0.02)	17.18(0.02)	16.86(0.02)
10432.7	18.91(0.03)	18.32(0.02)	17.39(0.01)	17.04(0.02)

Table 25: Photometry of SN 1996blk

JD (2440000+)	B (mag)	V (mag)	R (mag)	I (mag)
10373.6	15.20(0.03)	14.54(0.02)	14.28(0.01)	14.36(0.02)
10374.6	15.27(0.02)	14.49(0.02)	14.30(0.01)	14.29(0.03)
10398.0	17.76(0.05)	16.33(0.03)	15.90(0.05)	—
10400.0	17.94(0.11)	—	—	—
10405.0	18.00(0.02)	16.60(0.02)	16.27(0.02)	15.87(0.02)
10408.0	18.00(0.04)	16.93(0.06)	16.38(0.02)	16.16(0.03)
10425.0	18.43(0.02)	17.31(0.02)	17.10(0.03)	16.72(0.03)
10521.0	20.41(0.03)	19.81(0.14)	20.69(0.25)	18.83(0.22)

Table 26: Photometry of SN 1996bv

JD	B	V	R	I
10408.9	15.88(0.01)	15.53(0.01)	15.29(0.01)	15.52(0.02)
10409.9	15.93(0.01)	15.57(0.01)	15.40(0.01)	15.56(0.02)
10411.9	16.03(0.01)	15.60(0.01)	15.44(0.01)	15.69(0.02)
10413.0	16.13(0.01)	15.70(0.01)	15.54(0.01)	15.78(0.02)
10420.1	16.73(0.01)	—	—	15.94(0.03)
10426.0	17.45(0.01)	16.35(0.01)	16.04(0.01)	—
10429.8	—	—	16.11(0.01)	15.87(0.02)
10451.8	18.78(0.07)	17.57(0.01)	17.06(0.02)	16.77(0.02)
10486.6	19.18(0.05)	18.32(0.01)	17.84(0.04)	—

Table 27: Photometry of SN 1996ai

JD (2440000+)	B (mag)	V (mag)	R (mag)	I (mag)
10254.0	16.95(0.02)	15.30(0.02)	14.52(0.02)	13.98(0.02)
10255.0	16.97(0.02)	15.29(0.02)	14.50(0.02)	14.02(0.02)
10256.0	16.97(0.02)	15.27(0.02)	14.47(0.02)	—
10257.0	17.01(0.02)	15.27(0.02)	14.48(0.02)	—
10258.0	17.00(0.02)	15.23(0.02)	14.49(0.02)	14.09(0.02)
10259.0	17.04(0.02)	15.29(0.02)	14.51(0.02)	14.18(0.02)
10260.0	17.06(0.02)	15.26(0.02)	14.53(0.02)	14.19(0.02)
10274.0	18.17(0.05)	16.03(0.11)	15.15(0.03)	14.53(0.02)
10276.0	—	—	15.33(0.09)	—
10278.0	—	15.96(0.02)	15.16(0.03)	14.52(0.02)
10281.0	18.99(0.05)	16.40(0.02)	15.24(0.02)	—
10282.0	18.99(0.02)	16.43(0.02)	15.26(0.02)	—
10283.0	19.13(0.05)	16.36(0.02)	15.30(0.02)	14.34(0.02)
10285.0	—	16.37(0.03)	15.30(0.05)	14.51(0.02)
10295.0	20.15(0.14)	17.11(0.03)	16.02(0.03)	15.04(0.02)

Table 1: SN Ia Photometry Comparisons

	FLWO-CTIO(SN 1994D)			
	B	V	R	I
$B_{max} \pm 10$ days	0.024(0.006)	-0.002(0.006)	-0.018(0.006)	0.008(0.006)
all	0.038(0.004)	-0.013(0.004)	-0.015(0.004)	-0.028(0.004)
FLWO-CPO(SN 1995D)				
	B	V	R	I
$B_{max} \pm 10$ days	-0.016(0.021)	0.002(0.021)	-0.066(0.021)	-0.029(0.021)
all	-0.011(0.011)	-0.003(0.011)	-0.047(0.011)	-0.046(0.011)

Table 2: Photometry of Comparison Stars

Field	Star	<i>B</i>	<i>V</i>	<i>R</i>	<i>I</i>
SN 1993ac	1	16.648	—	—	—
	2	17.862	17.067	16.605	16.134
	3	18.714	17.968	17.497	17.030
	4	19.189	18.187	17.632	17.131
SN 1993ae	1	18.271	17.351	16.861	16.335
	2	17.080	15.835	15.076	14.344
SN 1994ae	1	13.427	12.577	12.093	11.797
	2	16.828	15.841	15.270	14.902
	3	15.531	14.599	14.016	13.596
	4	16.125	15.074	14.479	16.014
SN 1994M	1	14.197	13.194	12.684	12.321
	2	15.091	14.464	14.084	13.688
SN 1994S	1	16.248	15.574	15.199	14.843
	2	16.352	15.181	14.408	13.766
	3	14.844	14.205	13.829	13.473
SN 1994T	1	16.663	15.982	15.590	15.195
	2	17.610	16.772	16.270	15.833
	3	18.548	17.822	17.420	16.902
	4	15.178	14.543	14.163	13.777
SN 1994Q	1	15.648	15.183	14.894	14.615
	2	14.768	14.207	13.868	13.550
	3	18.048	17.041	16.424	15.964
SN 1995D	1	15.018	14.321	—	13.665
	2	15.397	14.679	14.262	13.919
	3	15.052	14.136	—	—
	4	16.651	15.895	15.453	15.109
	5	15.044	14.381	14.005	13.687
SN 1995E	1	16.627	16.038	15.718	15.389
	2	18.288	16.927	16.106	15.334
	3	18.243	17.388	16.826	16.389
	4*	15.401	14.902	14.562	14.276
SN 1995al	1*	15.164	14.600	14.273	13.931
	2	14.757	13.901	13.499	13.086
	3	15.439	14.756	14.394	14.019
	4	14.978	14.146	13.925	13.380
SN 1995ac	1	16.267	15.533	15.092	14.540
	2	17.412	16.781	16.386	15.924
	3	18.614	17.958	17.492	16.517
	4	19.573	18.491	17.592	16.517
SN 1995ak	1	16.416	15.627	15.160	14.804
	2	17.115	15.585	14.632	—
	3	16.403	15.556	15.044	14.696

* primary comparison star for field

Field	Star	<i>B</i>	<i>V</i>	<i>R</i>	<i>I</i>
SN 1995bd	1	16.407	15.429	—	—
	2	16.053	14.675	—	—
	3	17.877	16.570	15.734	14.943
	4	17.923	16.651	15.905	15.227
SN 1996C	1	17.390	16.693	16.343	16.004
	2	17.592	16.491	15.912	15.393
	3	17.298	16.341	15.805	15.432
	4	15.526	14.891	14.526	14.190
	5	15.346	14.396	13.934	13.505
SN 1996X	1	14.427	13.697	13.370	13.066
	2	15.168	14.134	14.029	13.978
	3	14.615	13.943	13.620	13.265
	4	14.483	13.837	13.526	13.180
SN 1996Z	1	14.704	14.194	13.909	—
	2	15.871	15.139	14.755	—
	3	15.931	14.952	14.382	—
	4	16.000	15.269	14.894	—
SN 1996ab	1	18.498	17.713	—	—
	2	20.487	19.839	—	—
	3	21.283	19.970	—	—
	4	19.605	18.814	—	—
	5	20.326	19.720	—	—
SN 1996ai	1	15.836	15.279	—	—
	2	16.347	15.801	15.524	—
	3	17.463	16.191	15.454	—
	4	17.407	16.740	16.410	16.003
	5	17.824	17.409	17.165	16.844
SN 1996bk	1	16.451	15.805	15.440	15.015
	2	16.907	15.839	15.293	14.763
	3	16.723	15.888	15.332	14.834
SN 1996bl	1	17.273	16.405	15.914	15.450
	2	17.845	17.224	16.873	16.478
	3	18.524	17.569	17.022	16.531
	4	18.422	17.345	16.666	15.968
SN 1996bo	1	17.030	16.30	16.791	15.382
	2	18.697	17.767	17.116	16.649
	3	17.991	17.125	16.556	16.131
	4	17.885	17.181	16.707	16.349
SN 1996bv	1	16.173	15.615	15.276	14.895
	2	17.618	16.858	16.427	15.966
	3	17.080	16.369	15.955	15.503
	4	18.390	17.774	17.408	17.000

* primary comparison star for field

Table 3: SN Ia Data

SN Ia	log cz	$^*B_{max}$	$^*V_{max}$	$^*\Delta_{m15}(B)$	1st Obs.	R. A. (1950.0)	Dec. (1950.0)	Photometry
1993ac	4.170	18.36	18.26	—	+6.0	05 41 37.0	+63 20 57.2	PSF
1993ae	3.757	15.46	15.50	—	+10.1	01 27 16.1	-02 14 05.5	PSF
1994M	3.838	16.31	16.28	—	+3.3	12 28 35.0	+00 52 53.4	PSF
1994S	3.658	14.80	14.85	—	-4.1	12 3 53.0	+29 24 37.4	PSF
1994T	4.017	17.31	17.24	—	+3.2	13 18 56.2	-01 53 15.0	PSF
1994Q	3.939	16.35	16.37	—	+8.6	16 48 11.6	+40 31 1.0	Gal. Sub.
1994ae	3.107	13.20	13.14	—	-12.0	10 44 23.0	+17 32 18.0	Aperture
1995D	3.293	13.42	13.43	—	-5.9	09 38 17.5	+05 22 6.6	Aperture
1995E	3.540	16.81	16.09	—	-0.3	07 46 7.9	+73 08 13.7	Gal. Sub
1995al	3.188	13.36	13.25	—	-4.1	09 47 59.5	+33 47 20.0	PSF
1995ak	3.839	16.23	16.13	—	+2.4	02 43 6.0	+03 01 15.0	Gal. Sub.
1995ac	4.176	17.23	17.21	—	-4.9	22 42 57.7	-09 00 44.4	Gal. Sub.
1995bd	3.681	17.29	16.51	—	-8.1	04 42 35.0	+10 58 36.6	Gal. Sub.
1996C	3.948	16.53	16.52	—	+3.9	13 49 1.4	+49 35 25.7	PSF
1996X	3.308	13.28	13.21	—	-3.2	13 15 16.2	-26 34 58.6	Aperture
1996Z	3.357	14.63	14.24	—	+4.6	09 34 26.3	-20 54 12.0	PSF
1996ab	4.571	19.47	19.51	—	+0.8	15 19 1.9	+28 06 20.8	Gal. Sub.
1996ai	2.978	16.94	15.26	—	-1.8	13 08 39.6	+37 19 31.5	Gal. Sub.
1996bk	3.310	14.89	14.52	—	+7.6	13 45 18.3	+61 13 9.6	Gal. Sub.
1996bl	4.033	17.05	16.96	—	-3.2	00 33 42.3	+11 07 9.9	Gal. Sub.
1996bo	3.714	16.17	15.76	—	-5.3	01 45 43.01	+11 16 20.9	Gal. Sub.
1996bv	3.700	15.38	15.28	—	+4.9	06 11 56.3	+57 04 10.5	Gal. Sub.

* Fit differently than Hamuy et al. 1996b. Only in Journal

Table 4: Galaxy Data

SN Ia	Galaxy	Type	$B - V$	North	galaxy offset East
1993ac	anon	E	1.11	31.0''	-5.3''
1993ae	UGC 1071	E	0.96	22.7''	16.1''
1994M	NGC 4493	E	1.09	-28.2''	3.4''
1994S	NGC 4495	Sbc	0.81	-6.9''	-14.0''
1994T	anon	Sa	1.03	-12.0''	3.8''
1994Q	anon	S0	0.66	-3.7''	-0.1''
1994ae	NGC 3370	Sc	0.78	6.1''	-29.7''
1995D	NGC 2962	S0	1.06	-87.8''	11.8''
1995E	NGC 2441	Sb	0.93	-20.8''	7.6''
1995al	NGC 3021	S	0.69	-3.1''	-14.7''
1995ak	IC 1844	S	0.72	0.8''	-7.1''
1995ac	anon	S	1.04	-1.4''	-0.9''
1995bd	UGC 3151	S	1.35	-1.0''	22.9''
1996C	MCG +08-25-47	Sa	0.81	13.2''	-1.8''
1996X	NGC 5061	E0	0.97	-31.7''	-51.4''
1996Z	NGC 2935	Sb	0.88	-69.9''	2.0''
1996ab	anon	S	0.85	0.6''	2.0''
1996ai	NGC 5005	SBcd	0.87	2.9''	23.3''
1996bk	NGC 5308	S0	0.52	-9.7''	-18.1''
1996bl	anon	SBc	0.82	5.6''	-3.2''
1996bo	NGC 673	Sc	0.62	-2.1''	6.7''
1996bv	UGC 3432	S	0.76	2.0''	-2.0''

Table 5: Discovery Data

SN Ia	discoverer (IAUC)	method	date	spectral i.d.
1993ac	J. Mueller (5879)	photo	10/13/93	J. Huchra, J. Brodie
1993ae	C. Pollas (5888)	photo	11/11/93	E. Cappellaro, A. Bragaglia
1994M	P. Wild (5982)	photo	04/30/94	J. Peters
1994S	B. Skiff (6005)	visual	06/04/94	J. Wheeler et al.
1994T	J. Peters, P. Challis (6007)	visual	06/11/94	J. Peters, P. Challis
1994Q	C. Pollas (6001)	photo	06/03/94	A. Filippenko et al.
1994ae	S. Van Dyk et al. (6105)	CCD	11/3/94	T. Iijima et al.
1995D	R. Kushida (6134)	CCD	02/10/95	S. Benetti et al.
1995E	A. Gabrielcic (6137)	CCD	02/21/95	P. Molare et al.
1995al	S. Pesci, P. Mazza (6255)	visual	11/01/95	J.-y. Wei et al.
1995ak	C. Pollas (6254)	photo	10/27/95	E. Cappellaro, M. Turatto
1995ac	C. Pollas (6237)	photo	09/23/95	A. Filippenko, D. Leonard
1995bd	C. Pollas (6278)	photo	12/20/95	P. Garnavich, A. Riess, R. Kirshner
1996C	J. Mueller (6317)	photo	02/15/96	P. Garnavich, A. Riess, and R. Kirshner
1996X	R. Evans, K. Takamizawa (6380)	visual	04/13/96	S. Benetti et al.
1996Z	W. Johnson (6401)	CCD	05/16/96	S. Benetti et al.
1996ab	J. Mueller (6405)	photo	05/12/96	P. Garnavich et al.
1996ai	C. Bottari (6422)	CCD	06/17/96	P. Challis et al.
1996bk	P. Mazza, S. Pesci (6491)	visual	10/13/96	P. Garnavich, R. Kirshner
1996bl	C. Pollas (6492)	photo	10/12/96	P. Garnavich et al.
1996bo	W. Li et al. (6497)	CCD	10/23/96	M. Turatto, S. Benetti
1996bv	W. Li et al. (6508)	CCD	11/3/96	W. Li et al.